Engineering Research Journal

journal homepage: https://erj.journals.ekb.eg/

Pounding among adjacent MRF multi-story buildings with open first storey and different floor heights

Abbas Moustafa [1], Magdy Genidy[2], Hesham Tahon[3,*], Hany Ragab[4]

[1] Professor, Civil Engineering Department, Faculty of Engineering, Minia University
[2] Associate Professor of R.C. Structures, Faculty of Engineering, Mataria, Helwan University
[3]Ph.D. Student, Civil Engineering Department, Faculty of Engineering, Mataria, Helwan University
[4]Assistant Professor, Construction Department, Faculty of engineering, Egyptian Russian University

[*]Corresponding author E-mail: hishamd01248@m-eng.helwan.edu.eg@gmail.com

Abstract. The primary objective of this paper is to assess the seismic response of neighboring colliding buildings with insufficient separation distances. Infill masonry panels significantly influence the overall behavior and seismic response of multistory moment-resisting frames (MRFs), particularly in the common scenario of a soft first story. A numerical simulation was conducted on a 12-story reinforced concrete (RC) frame, along with one-story and 6-story buildings. Dynamic nonlinear time-history analyses, using three ground motion records from near-fault and far-fault regions, were performed to evaluate the seismic response of the considered model configurations. The study focuses on the seismic interaction among adjacent buildings of varying heights and different story levels, including a soft story at the first floor (pilotis). The terms "pilotis frame" or "pilotis configuration" refer to RC structures with fully infilled upper levels while leaving the ground level open without infill. Two pounding scenarios were examined in all interacting buildings: Case A (slab-to-slab) and Case B (slab-to-column). Two configurations were considered: a fully infilled 12-story frame and an infilled 12-story frame with a soft first floor. Additionally, two directions of excitation (positive and negative) were analyzed, as they significantly influence the buildings' responses due to the asymmetry of the adjacent building pairs. Structural response parameters include story displacement, inter-storey drift, induced pounding force, hysteresis loops, and the performance level of plastic hinges in the ground columns. The results indicate that the pilotis arrangement significantly amplifies the first inter-storey drift and induced pounding force. Case B pounding has a more pronounced effect on the adjacent buildings' responses and causes greater permanent deformation compared to Case A pounding. The severity of seismic pounding depends on the properties of each building, the characteristics of the input excitation, the configuration of infill panels, and the direction of the input excitation.

Keyword: Seismic pounding, ETABS software, Soft storey, Slab to column pounding, Permanent deformation, Nonlinear dynamic time history analysis, Pilotis, Plastic hinges.

1. Introduction

Due to field investigations following catastrophic earthquakes and the fundamental findings reached thus far from several reports, it recognized that damage during seismic activity often results from interactions between adjacent buildings [1]. Another name for this phenomenon is structural pounding,

DOI: 10.21608/erj.2025.403753.1266
Received 14 July 2025; Received in revised form 07 August 2025; Accepted 18 August 2025
Available online 01 September 2025

which occurs when buildings come into contact with each other or are near one another. Earthquake investigators have frequently documented pounding throughout the earlier few decades. It is clear from the vast amount of research that structural pounding was documented during the earthquake of Alaska 1964 and the earthquake of Managua 1972 [1]. Furthermore, as stated by Meli and Rosenblueth (1985) [2] and Bertero (1986) [3], the initial evaluation following in situ observations of the 1985 earthquake in Mexico showed that structural pounding was responsible for a significant portion (almost 40%) of the noted damage. This assessment, which was later substantially changed, found that the cooperation between structures was also responsible for a sizable portion of collapse cases. Additionally, the Loma Prieta earthquake showed the substantial seismic risk of structural pounding because several pounding incidents were documented in the densely populated Bay Region, in both Oakland and San Francisco, nearly 90 kilometers from the epicenter [4,5].

Although the damage and collapse incidents in the Loma Prieta and Mexico City earthquakes are distinct seismic events, Structural pounding is a common occurrence in all major earthquakes. There is usually structural pounding during large earthquakes, which leads to building damage and total collapse. Several cases of medium to significant damage due to structural pounding were also found in the Kalamata Greece 1986, Aegion Greece 1995 (Figure 1a), and Alkyonides Greece 1981 (Figure 1b) earthquake events [6].

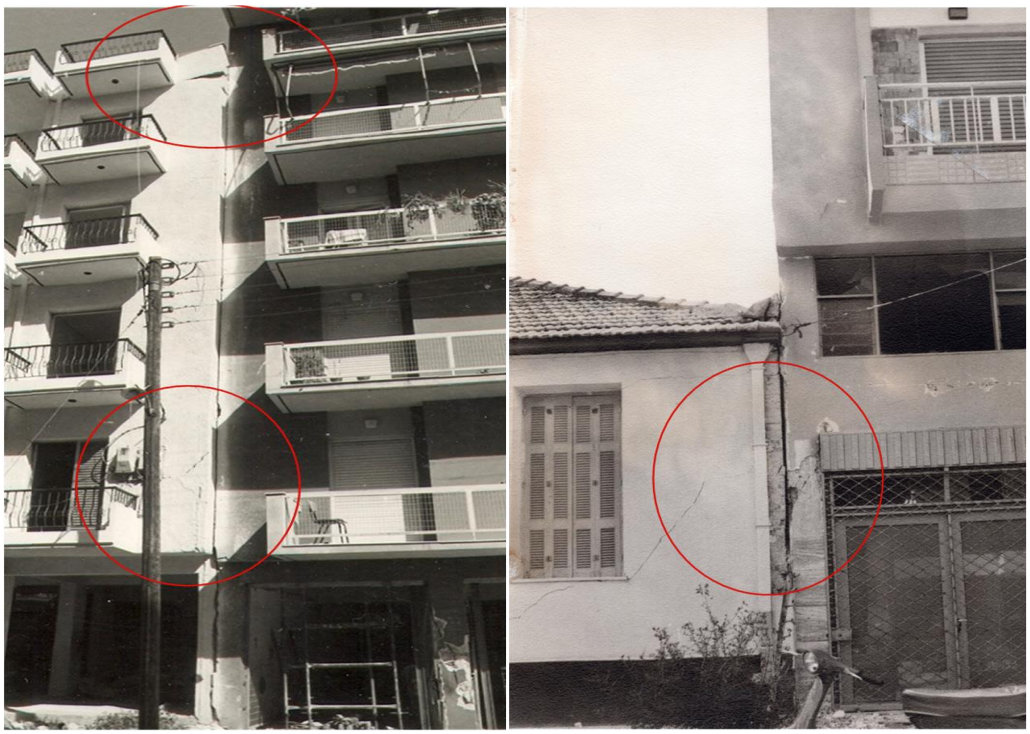

(a) (b)

Fig. 1 Pounding damage between adjacent structure (a) interaction among two multistorey pilotis buildings Case A (kalamata 1986), (b) interaction among multistorey totally infilled building and one-story building (Alkyonides 1981) [6]

To prevent buildings colliding, modern seismic codes like ECP-201 [7] recommend specific distances between neighboring buildings. However, a vast number of current buildings have been constructed adjacent to or in contact with each other. Furthermore, it is observed that the gap distances suggested by codes have no relation with the structural elements' local capacities that could be subjected to the pounding impact or the seismic hazard. Sometimes, these missed relation can result in inadequate

separations or not accordance with the modern codes that permit substantial deformations and, as a result, large lateral displacements during ground motion due to the principle of inelastic response.
For nearly thirty years, researchers have examined several facets of the issue interaction among neighboring buildings. The earliest research concentrated on the pounding interacting of s single-DOF systems during seismic excitations [8]. In order to precisely assess the structural pounding risk, the interaction of multi-storey R.C. structures was then investigated. According to these research, collisions occurred among the floors of the buildings (Case A pounding) because the colliding multi-storey structures had similar story heights [9–11]. Buildings colliding could result in increased storey accelerations, increased storey shear forces and increased inter-storey drifts. Additionally, it generates large pounding forces between the interacting structures, as well the storey displacements and roof displacement may rise noticeably. Abbas Moustafa and Sayed M. [12] used input energy, dissipated energy, and damage indices to evaluate the pounding of adjacent buildings.
Both fixed-base and isolated-base adjacent buildings are considered. Short-, moderate-, and long-duration accelerograms recorded at near-fault and far-fault regions with various soil classification are included in a group of ground excitations. It has concluded that adjacent buildings with isolated-base experience pounding force one to four times while adjacent buildings with fixed-base experience pounding force once or twice. Additionally, adjacent buildings with fixed base dissipate larger energy through hysteresis mechanism relative to adjacent buildings with base isolation.
The response of adjacent buildings is mainly amplified in the pounding direction. While the response of adjacent buildings in the other direction is usually unaffected unless the geometric plan of interacting buildings is asymmetric. Herein, the interacting structures experience torsional movements as a result of the non-symmetric pounding [13–15].
Mahmoud et al. (2016) [16] shows that the masonry infill mechanism has a considerable influence on the global performance of R.C. moment resisting frame buildings. The structural response of bare frame, in which action of masonry infilled is ignored, does significantly vary with the totally or partially infilled frame. Moreover, the infilled frame building models with soft storey (open storey or pilotis) have sudden increase in the structural response under all ground motion records. The study drew useful recommendation to be added to the national building codes. Magnification factor should be provided for storey shear forces and overturning moments responses for the column of the soft storey.
Structural pounding among three neighbouring structures side by side with various building height has been investigated by Moustafa et al. [17]. An analytical simulation of three neighbouring structures of 3-story, 6-story, and 12-story MRF are combined by nonlinear gap element and subjected to seismic excitation. It has been concluded that the significance of seismic pounding influence is assessed by the vibration properties of each building, the characteristics of input excitation, separation gap sizes, building height ratio, and the location of the structure in series: whether it is an edged building that could be pounded from one side or a middle building that could be struck from both sides.

2. Significance of Study

It was evident from the foregoing literature analysis that the problem of structures interaction has been extensively researched in the past. Nevertheless, some significant issues have not received any attention or have not been covered in depth. This study concentrates on a portion of them.
Initially, the stiffness and structural action of masonry infills wall has been ignored in most of the abovementioned literature studies. The primary goal of the current study is to examine the response of R.C. moment resisting frame buildings with pilotis-configuration getting pounded by shorter building. The response parameters of totally infilled buildings configuration are compared to the corresponding parameters of pilotis configurations.
Additionally, the directionality of seismic excitation is investigated. Only one direction of seismic excitation was taken into consideration when performing inelastic dynamic analysis in the previously

`

described studies. This would obviously make sense for symmetric structures. But pounding eliminates all symmetry. Both ground motion directions were considered in this research.
Finally, the current paper demonstrates the behaviour of hysteresis loops of edge columns that suffer collide from the slab of adjacent building (Case B pounding). Comparison between the case of totally infilled frame and case of pilotis has been examined and figure out.

3. Research methodology

Nonlinear dynamic time history analysis was used to investigate the influence of masonry panels and pilotis configuration on the buildings interaction of varying total heights. The following two cases of pounding were investigated:

1. pounding between structures with equal storey levels (Case A pounding).
2. pounding when the floor levels of the first and second structures differ, as a result the floors of each structure collide with columns of the other one (Case B pounding).

Additionally, the following two examples of masonry configuration were examined:

a. Completely infilled frame.
b. Completely infilled frame except the ground floor (pilotis).

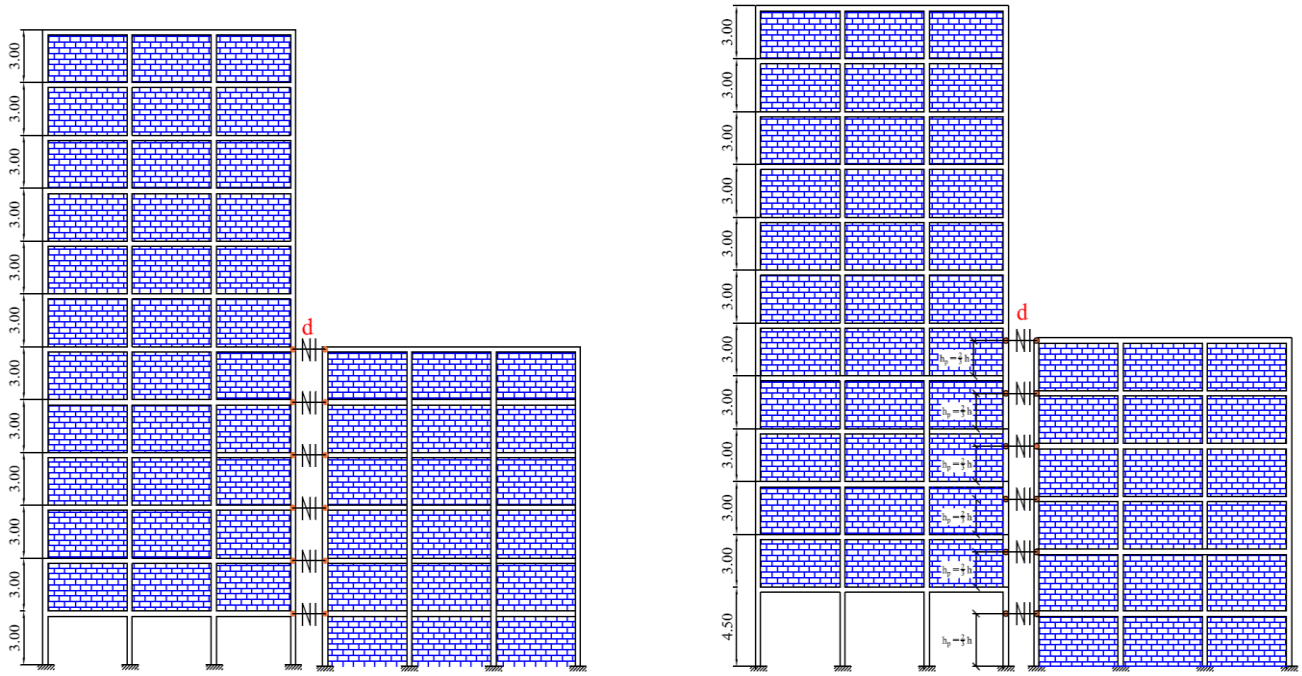

Fig. 2 (a) Case A or slab-to-slab pounding (b) Case B or slab-to-column pounding

These building models are subjected to strong earthquake excitations of El-Centro, near and far-fault regions of Loma Prieta. The gap distance between adjacent buildings named "d" is taken equal to zero (case of full contact). Nonlinear direct integration time-history analysis is carried out using the ETABS Ultimate C V20.3.0 Build 2929 [18]. Various responses quantities are assessed as relative displacements, induced impact force, hysteretic loops and inter-storey drifts.

4. Nonlinear building and pounding models' assumptions

4.1 Nonlinear Buildings models 'assumptions

The most effective method for assessing structures response to seismic excitations provided by ground acceleration records is time-history analysis method, which is a nonlinear dynamic analysis. The most powerful method for nonlinear analysis, Newmark time integration, is used to solve the governing equations of motion in a step-by-step nonlinear direct integration procedure. Dynamic earthquake loads gradually alter the structure with time intervals (Δt = 0.02 and 0.005 s). Series of short time increment are used to evaluate the structural response. For MDOF, the general equation of motion in incremental form is [19]:

$$\boldsymbol{M}\Delta\ddot{U}(t) + \boldsymbol{C}(t)\Delta\dot{U}(t) + \boldsymbol{K}(t)\Delta U(t) + F_p(t) = -\boldsymbol{M}\{\mathbf{1}\}\ddot{u}_g(t) \quad (1)$$

Where $\boldsymbol{M}$, $\boldsymbol{C}$ and $\boldsymbol{K}$ are stands for mass matrix, damping matrix and initial stiffness matrix respectively. The vectors U is displacement vector and dot indicate differentiation with respect to time. $\ddot{u}_g$ is the earthquake acceleration's single component. $\{1\}$ is a vector of ones. F_p is the force vector due to impact (pounding force) More sensible insight to the equation is presented by the equation no.2.

The coefficients multiplying the mass and stiffness matrices are calculated based on carefully selected frequencies of the studied buildings.

$$\begin{bmatrix} m_{xn} & 0 \\ 0 & m_{ym} \end{bmatrix}\begin{Bmatrix} \ddot{u}_{xn} \\ \ddot{u}_{ym} \end{Bmatrix} + \begin{bmatrix} c_{xn} & 0 \\ 0 & c_{ym} \end{bmatrix}\begin{Bmatrix} \dot{u}_{xn} \\ \dot{u}_{ym} \end{Bmatrix} + \begin{bmatrix} k_{xn} & 0 \\ 0 & k_{ym} \end{bmatrix}\begin{Bmatrix} u_{xn} \\ u_{ym} \end{Bmatrix} + \begin{Bmatrix} \overline{F}_{P1} \\ -\overline{F}_{P2} \end{Bmatrix} = -\begin{bmatrix} m_{xn} & 0 \\ 0 & m_{ym} \end{bmatrix}\begin{Bmatrix} 1 \\ 1 \end{Bmatrix}\ddot{u}_g(t) \quad (2)$$

Rayleigh damping of 5% damping ratio is adopted, the mass proportional coefficient a_0 (1/sec) and stiffness proportional coefficient a_1 (sec) are calculated based on carefully selected natural frequences of the studied buildings which extracted from the first, second and third mode shapes.
The nonlinear time history analysis of MRF building models has been performed using the structural program ETABS Ultimate C (Version 20.3.0 Build 2929). In terms of material and geometrical nonlinearities, nonlinear analysis is considered as a realistic structural analysis that can imitate the appropriate behaviour of the material and the deformation of structural elements under dynamic loads. The degrading of hysteretic loops used in this study is according to Takeda model. This model follows hysteretic rules for describing the nonlinear relation between the applied force and the corresponding deformation of the structural members. The figure illustration of the Force displacement relationships of Takeda hysteretic model is shown in Fig. 3. Fig. 4 displays the nonlinear stress-strain curves for both concrete and reinforcement rebars. Beam-column element's both ends have plastic hinges (flexural hinges in beams, biaxial axial-flexural hinges in columns) have been used for the structural members of the nonlinear models. Mander stress–strain curve is assigned to concrete material section for confined and unconfined compression and tension stress–strain relation [20].

`

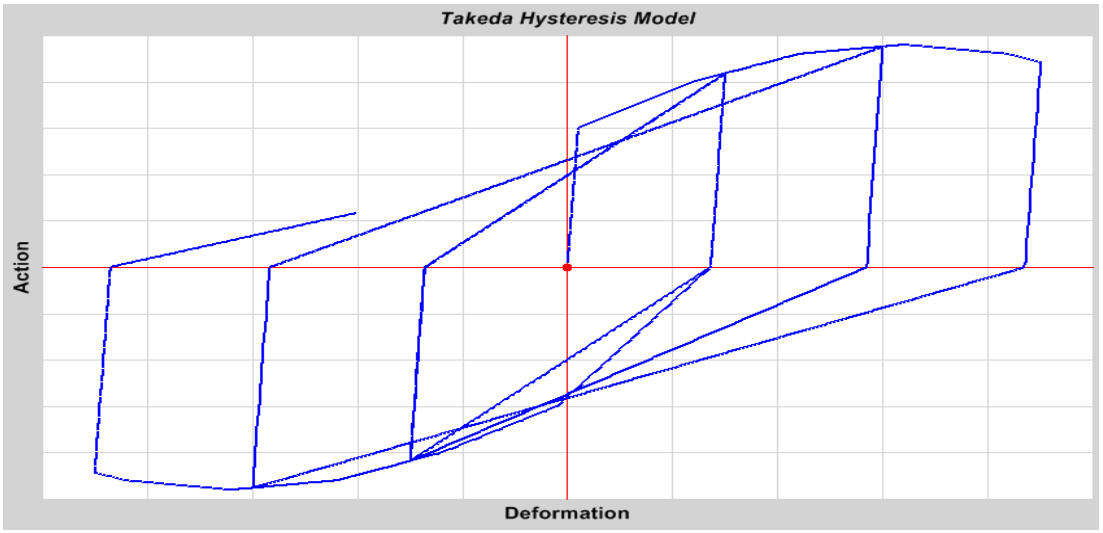

Fig. 3 Force-deformation relationship for Takeda hysteresis Model developed in ETABS.

The nonlinear parameters that contribute to sensitivity analysis are as follows: solution scheme is iteration only, maximum constant-stiffness iterations set to 10, maximum Newton-Raphson iterations set to 40, and a relative iteration convergence tolerance of 0.01. Line search has been enabled, with a maximum of 20-line searches per iteration.

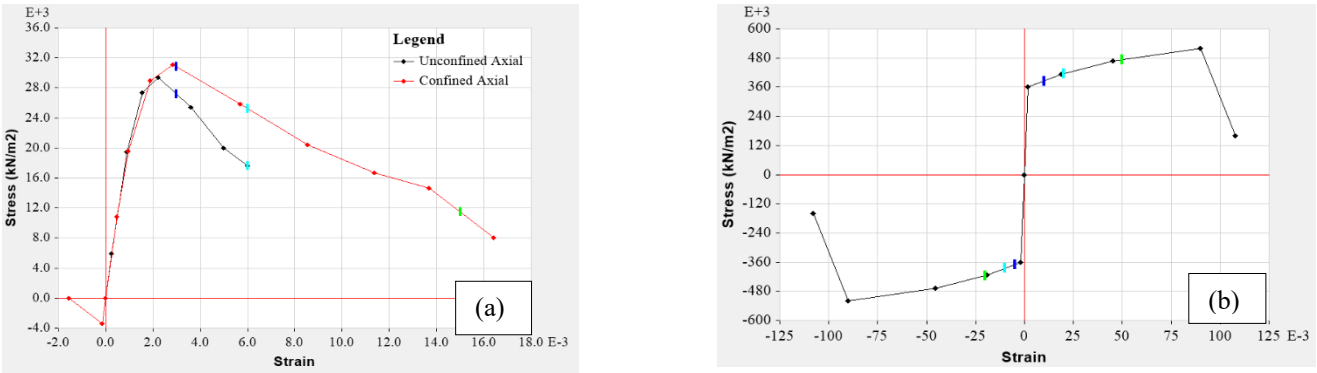

Fig. 4 Nonlinear stress strain curve for (a) concrete and (b) steel rebar used.

The yielding and post-yielding behaviour can be modelled using plastic hinges. According to ASCE 41-17 standards (ASCE 2017) [22] and FEMA-356 (FEMA 2000) [21], plastic hinge parameters can be automatically calculated from the elements' cross section, reinforcement ratio, stirrups and material properties. The fiber P-M2-M3 hinge models the axial behaviour of a number of representative axial fibers distributed across the cross section of the frame element.

4.2 Nonlinear pounding model assumptions

To simulating induced pounding force among adjacent structures, the gaps between the buildings are modelled by using compression only gap element as shown in Fig. 5. The pounding force of impact model $\overline{F}_P$ is determined as:

$$\overline{F}_P = \begin{cases} k\delta + c\dot{\delta}, & \delta \geq d \\ 0 & , \delta < d \end{cases} \quad \delta = u_i - u_j - d \,, \dot{\delta} = \dot{u}_i - \dot{u}_j \qquad (3)$$

where the relative displacement and relative velocity between the colliding structural elements are denoted by δ and $\dot{\delta}$. c, k, $\dot{u}_i$, $\dot{u}_j$, u_i, u_j and, d are the damping, stiffness, displacement, velocity of the element's nodes i, j and d is the separation gap for the impact model, respectively.

Different approaches to estimate the gap element stiffness have been examined in several studies. Based on the theory of wave propagation, Watanabe and Kawashima [23] conducted a mathematical model to determine the appropriate impact spring stiffness and the numerical integration time interval. Maison and Kasai [24] concluded that the impact stiffness can be described as the contact bodies' axial stiffness, and the stiffness gap element is equal to the floor's axial stiffness at the impact level. Gap element with a 20x amplification factor times the rigid SDOF system's lateral stiffness was presented [25]. At the present research, the gap element's impact stiffness "k" is calculated as the higher value of stiffer building's lateral stiffness at the impact level or the impacted floors' axial stiffness according to Eq.4. [26, 27].

$$k = \gamma \frac{EA}{b} \qquad or \qquad \gamma = \frac{3EI}{h^3} \qquad (4)$$

where, A, E, b, I and h are stands for the area of impact surface, elasticity modulus, width of building in the impact direction, stiffer building's moment of inertia as equivalent cantilever model and building height till the level of impact respectively. The stiffness amplification factor, $\gamma = 50$ is calculated based on a sensitivity study of the impact stiffness value. The damping constant c is used to account for energy dissipation during colliding. However, the acceleration response may be strongly influenced by overly large values of spring stiffness and may compromise the precision of the dynamic model response. The impact element uses the damping component to take into consideration how much energy is dissipated through each colliding. Reasonable values of this coefficient can be calculated by comparing it to the restitution coefficient, e, for two masses, m_x and m_y, colliding with arbitrary velocities [28].

$$c = 2\xi\sqrt{k\frac{m_x m_y}{m_y + m_y}} \quad \text{and} \quad \xi = \frac{-\ln e}{\sqrt{\pi^2 + (\ln e)^2}} \qquad (5)$$

The restitution coefficient varies from zero to one, which represents completely plastic impact to elastic impacts, respectively. For concrete buildings collisions, a coefficient of restitution about 0.65 (ξ = 0.14) has been utilized [28,29].

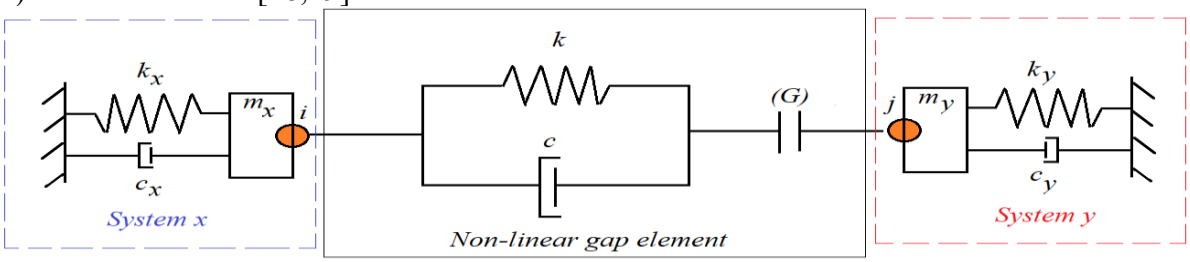

Fig. 5 Nonlinear gap element impact model between adjacent buildings

4.3 Simulation of masonry panels

The equivalent strut model has been utilized to simulate the action of masonry infills (Figure 6a). The literature in ref. [30] has looked at two main types of elements. The first type was a truss element that responded bilinearly in compression and had zero strength in tension. In this analytical procedure, it was assumed that the total infilled frame strength would match the bare frame strength if the truss element achieved its ultimate strength. The other type used in this paper more precisely accounts for the infill masonry's response. It has residual strength and a degrading branch (Figure 6b). Particularly, the axial behavior of the diagonal struts is described by the five points (A to E), and every point represents a unique state of strut. A is the first yield point, B is an intermediate point between A and B where a notable decrease in stiffness takes place, C indicates the strut's maximum strength, whereas the degrading and residual strength branches begin at points D and E, respectively. It was crucial that both diagonal struts indicate compression response only and without any flexural behavior.

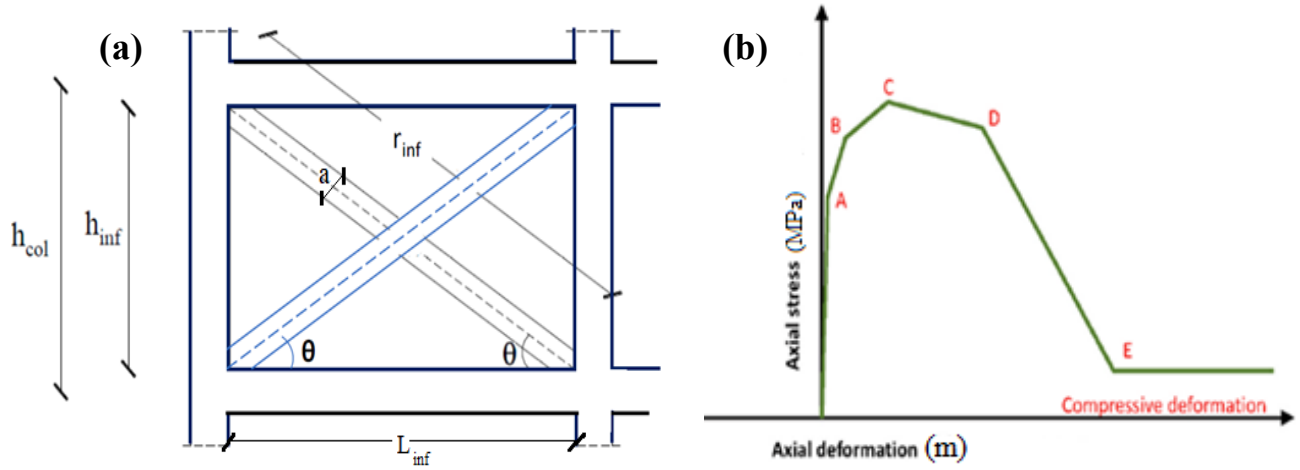

Fig. 6 Simulation of masonry infill panel (a) Double diagonal struts model (b) Bilinear axial compression response.

In the current research, walls are modelled as solid panels without opening. The masonry infill walls will be modeled in accordance with FEMA 356 [21]. The modulus of elasticity and thickness of masonry panel are 5500 MPa and 0.20 m respectively.

Masonry infill walls prior to cracking are modelled using an equivalent double diagonal compression strut with width, a, according to FEMA 356. The strut and the infill panel are identical in terms of elastic modulus and thickness. The strut's thickness can be expressed in the form of the column height h_{col} between centerlines of beams and the length of panel is L_{inf}. Equation (6) provides an equivalent diagonal compression strut of width (a) that represents the elastic in-plane stiffness of a solid unreinforced masonry infill panel before it cracks.

$$a = 0.175(\lambda_1 h_{col})^{-0.4} r_{inf} \tag{6}$$

Where the value of diagonal length of infill panel r_{inf} can be calculated according to Eq. (7).

$$r_{inf} = \sqrt{(L_{inf})^2 + (h_{inf})^2} \tag{7}$$

The Coefficient λ_1, which is used to calculate equivalent width of infill strut, can be calculated as a variable of the infill panel height h_{inf}, modules of elasticity of both frame materials E_{fe} and material of infill panel E_{me}, columns moment of inertia I_{col}, infill panel length L_{inf} and thickness t_{inf}, according to Eq. (8):

$$\lambda_1 = \left[\frac{E_{me}\, t_{inf} \sin 2\phi^{\circ}}{4E_{fe} I_{col} h_{inf}}\right]^{\frac{1}{4}} \tag{8}$$

4.4 Physical building model

Both neighboring buildings models connected with non-linear gap element with various total heights have been investigated. One of these structures is multistorey totally infilled-frame structure or an infilled-frame structure with a soft first story (open storey or pilotis) which is in contact with one-storey structure or shorter structure. The distance between structures shall be defined as (d). This study investigated how pre-existing (d) size affects pounding effects. Two different types of building interactions were discovered as follows:

(a) Figures 8a and 9a depict Case A pounding, often known as slab-to-slab pounding. Collisions occur between floor slabs in interacting structures due to their equal heights.
(b) Case B pounding, also known as slab-to-column pounding (Figures 8b and 9b). In this scenario, the interacting buildings' floor levels varied. As a result, collisions occur between slabs and columns. Both frames' slabs collided with the other's column. The impact between a taller frame's column and the upper floor of a shorter building can be severe and perhaps fatal.

Columns' cross section dimension and reinforcement of 12-storey and 6-storey buildings are shown in table1. The pounding cases under consideration included the interaction among a 12-story MRF structure with (a) a one-story structure (Figure 8) and (b) a 6-story structure (Figure 9). Every pounding case was examined for slab-to-slab interaction (Case A) and slab-to-column interaction (Case B). In addition, the 12-story MRF was assumed (a) as a frame with totally infilled and (b) as totally infilled frame with a soft storey. Noting at the infilled frames, the infill walls have been considered at all beam's lines at both directions.

`

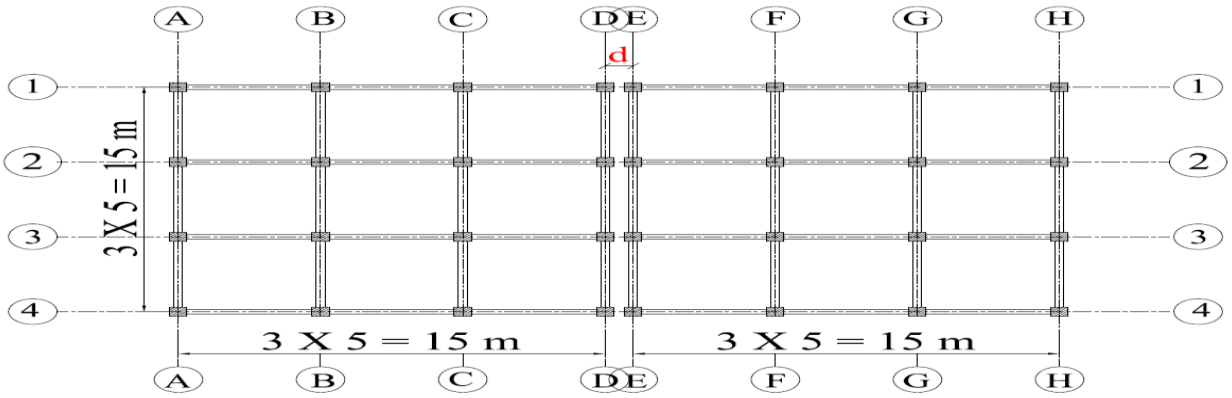

Fig. 7 Typical floor plane for 12-story building and 6-story or one-story building

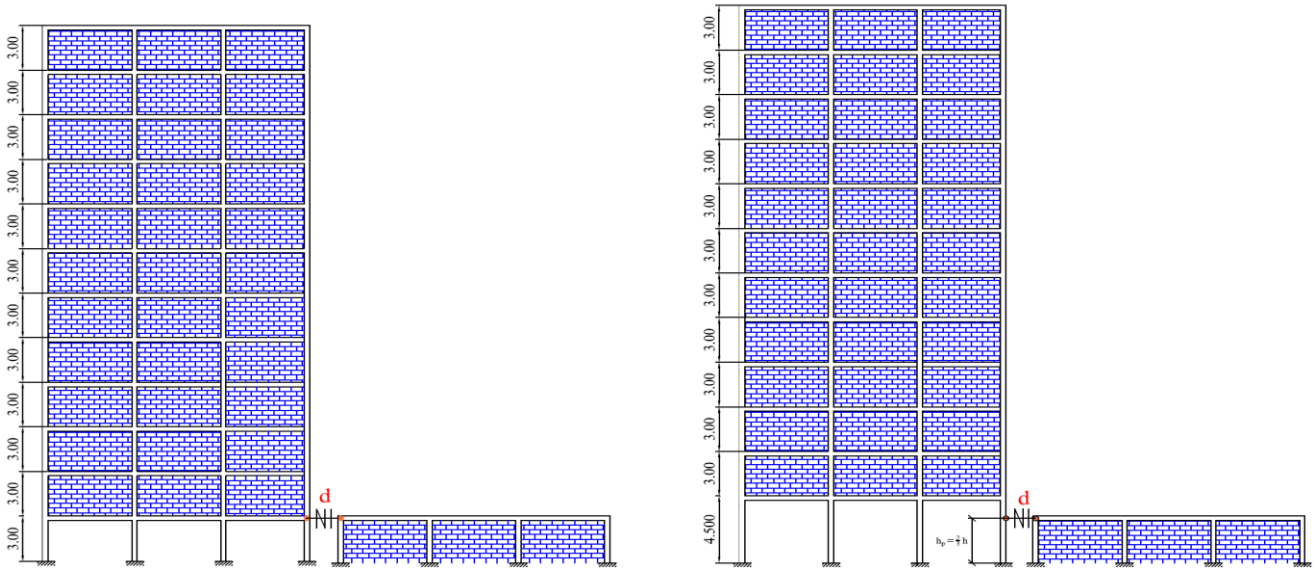

Fig. 8 Seismic pounding between 12-storey pilotis frame and an infilled one-storey structure (a) Case A or slab-to-slab pounding (b) Case B or slab-to-column pounding

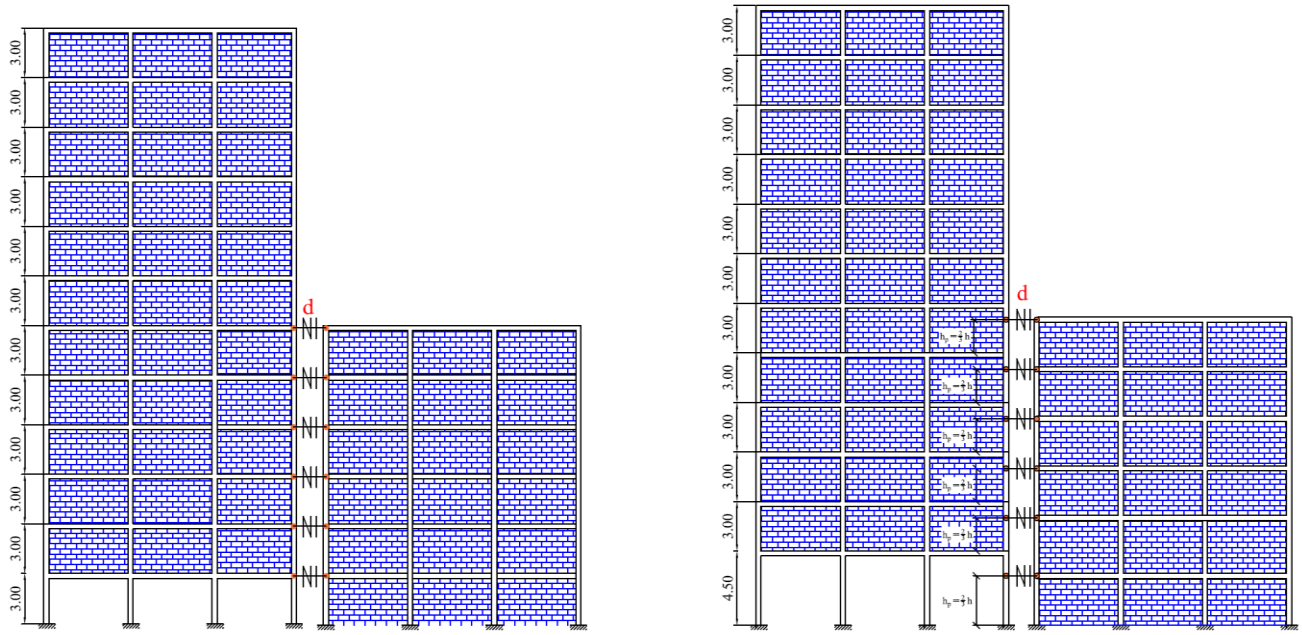

Fig. 9 Seismic pounding between 12-storey pilotis frame and 6-storey infilled-structure (a) Case A or slab-to-slab pounding (b) Case B or slab-to-column pounding

The three models for typical buildings with one, six and twelve stories are selected as depicted in Figures. 8 and 9. The buildings have typical floor plan with bay width 5 m in each direction (fig. 7). f_c = 30 MPa, unit weight = 25 kN/m^3, modulus of elasticity E_c = 24 GPa, Poisson's ratio υ = 0.2 and reinforcing steel with yield strength F_y = 360 MPa are used for analysis and design. The dead loads take account of the own weight of the structural components; the weight of flooring cover (1.5 kN/m^2) and panel wall loads intensity of 10 kN/m on all beams. The residential buildings are chosen to have a live load of 2 kN/m^2. The floor has 0.15 m slab thickness and 0.3 × 0.7 m dropped beam with equally top and bottom reinforcement 5T12 and 5T8/m confinement stirrups. The dimensions and reinforcement of column elements for the studied buildings are presented in Table 1.

Table 1 Cross-sections dimension (m) and rebar for column of the buildings model

Building	Column location	Story No.			
		From 1 to 3	From 4 to 6	From 7 to 9	From 10 to 12
		Dimension Reinforcement	Dimension Reinforcement	Dimension Reinforcement	Dimension Reinforcement
12-Story	Corner	0.60 × 0.60 26T20	0.50 × 0.50 22T18	0.50 × 0.50 22T14	0.40 × 0.40 22T14
	Edge	0.70 × 0.70 26T20	0.60 x 0.60 22T20	0.50 × 0.50 22T18	0.40 × 0.40 22T14
	Interior	0.80 × 0.80 30T22	0.70 x 0.70 28T22	0.60 × 0.60 26T20	0.50 × 0.50 22T20
6-Story	Corner	0.50 × 0.50 22T14	0.40 x 0.40 22T14		
	Edge	0.50 × 0.50 22T18	0.40 x 0.40 22T14		
	Interior	0.60 × 0.60 26T20	0.50 x 0.50 22T20		

5. Ground excitations.

Three different ground excitations have been selected to perform the dynamic analysis of the current study. One of these records is the El-Centro with site source distance of about 8 km. The second and third records have been taken from the near and far-fault regions of Loma Prieta. Figure 10 provides the acceleration time-histories and Fourier amplitudes for the three earthquake ground motions used in the current study. The PEER Strong Motion Database is the source of the ground seismic excitation (http://peer.berkeley.edu/smcat/) [31]. Dynamic earthquake loads gradually alter the building with time intervals (Δt equal to 0.02 sec) for the El-Centro 1940 record while time intervals (Δt equal to 0.005 sec) for the Loma Prieta 1989 both records. Table 2 show the ground motions parameters as, recording station, soil class, magnitude, peak ground acceleration (PGA), site to source distance and total duration.

Table 2 Ground motion records used as input to adjacent buildings.

Earthquake (record)	Date	Soil Class	Station	PGA (g)	M	D_{ss} (km)	t_d (s)
El Centro (180)	05.19.1940	D	117 El Centro	0.34	7.2	8.3	53
Loma Prieta NF (090)	10.18.1989	B	Corralitos	0.48	7.1	5.1	40
Loma Prieta FF (285)	10.18.1989	A	Coyote Lake Dam	0.48	7.1	21.8	40

Soil class = geomatrix soil class, USGS, PGA = peak ground acceleration, M = magnitude, D_{ss} = site–source distance, t_d = earthquake total duration.

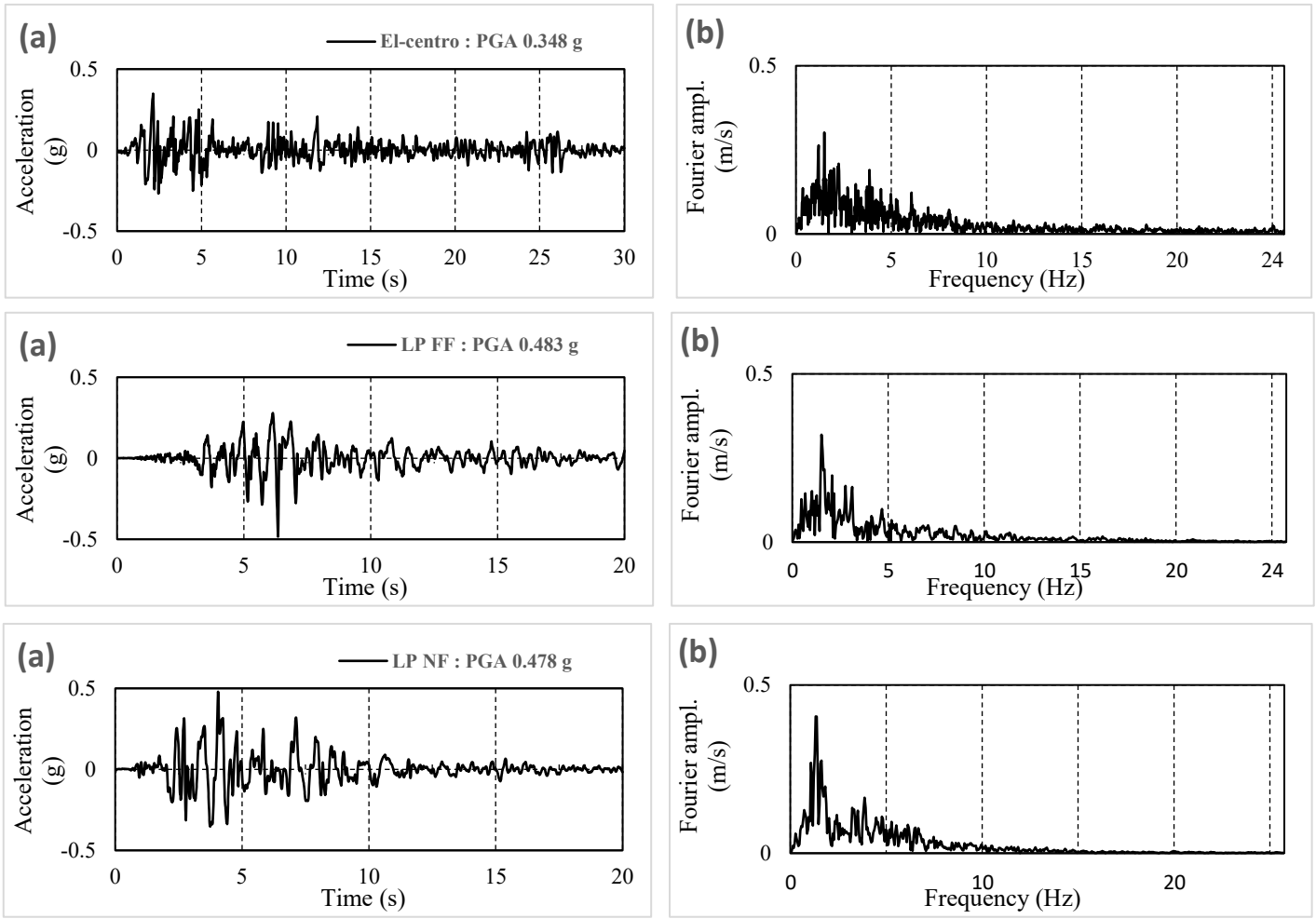

Fig. 10 Ground excitation record to adjacent structures (a) Acceleration time histories (b) Fourier amplitude [31]

6. Numerical results and discussion

6.1 Analysis of natural vibration of buildings

Table 3. fundamental natural time periods for different buildings model to perspective vibration mode

Model Type	Natural period (sec.) (ETABS 3-D FE dynamic analysis)		
	12- storey building	6- storey building	one- storey building
Bare frame	1.560	0.896	0.138
Infilled frame	0.765	0.340	0.069
Pilotis frame	0.810	0.374	0.076

Table 3 shows fundamental natural time period for different infill configurations in addition to bare frame for the three buildings model. It observed that the model of bare frame, which masonry infills action has been ignoring, gives a higher time period relative to the other models under consideration. The percentage changes in lateral natural period due to incorporation of the masonry infill walls represented by infilled frame in the Table 2 compared to the lateral natural period of bare frame model is about 50%.

6.2 Pounding between 12-stroey and one-storey buildings

Interaction cases among the 12-storey frame and one-storey frame at the impact level of first floor were investigated considering the pounding configuration as depicts in figure 8: (a) floor-to-floor pounding (case A) (b) floor-to-column pounding. All interaction cases were exposed to three ground motions of El-Centro, near fault and far fault of Loma Prieta and every ground motion was utilized two times in positive and negative directions see figure 11.

6.2.1 Slab-to-slab interaction (Case A)

Figures 12, 13, 14, 15 and 16 display the slab-to-slab pounding results for the 12-story building and an infilled one-story considering the 12-story building was completely infilled or partially infilled with an open storey at first floor. The first-floor displacement as a function of time history for the interaction of case (i) completely infilled building with an infilled one-storey (red dot line) with case (ii) pilotis arrangement (black continuous line) are depicts in figures 12 and 13. Figure 12 represents the time histories displacement of the first storey of 12-storey building subjected to El-Centro record which utilized in the global positive direction of adjacent building (i.e. from left to right). The pilotis configuration considerable rise the first storey displacement compared to the infilled configuration under El-Centro record. Compared to storey displacement under El-Centro record, the storey displacement under Loma Prieta NF record considerable higher regardless of the infilled or pilotis configuration. It was noticed from figure 13 that frame pilotis configuration could cause significant permanent deformation, especially after 12 secs of excitation start under Loma Prieta NF record.

In Figures 14, 15 and 16, the maximum inter-story drifts of the 12- story frame for slab to slab pounding case under three excitation record applied in both positive and negative directions are also presented. It was noticed that the pilotis arrangement raised the inter-story drift of the open storey and result in significant inelastic (permanent) deformations due to the buildings interaction. On the contrary, there was no significant difference in the inter-storey drifts of the top stories especially under positive excitation of El-Centro and negative excitation of Loma Prieta FF. However, there are notable differences in the inter-story drifts of the top stories of the 12-story structure between the considered cases under the Loma Prieta NF record. Additionally, there are significant variations in responses between the positive and negative directions of input excitation. The worst case of pilotis arrangement can be noticed under the negative direction of El-Centro excitation where the magnification in inter-story drifts reach to 220 %.

6.2.2 Slab-to-column interaction (Case B)

The schematic in Figure 17 illustrates both the positive and negative directions of each seismic excitation for Case B pounding. Figures 18, 19, 20, 21, and 22 show the slab-to-column pounding results for a 12-story frame and a one-story infilled frame with a floor height below the first story height of the 12-story frame considering the 12-story frame can be either (a) completely infilled or (b) pilotis (infilled frame with open story)

`

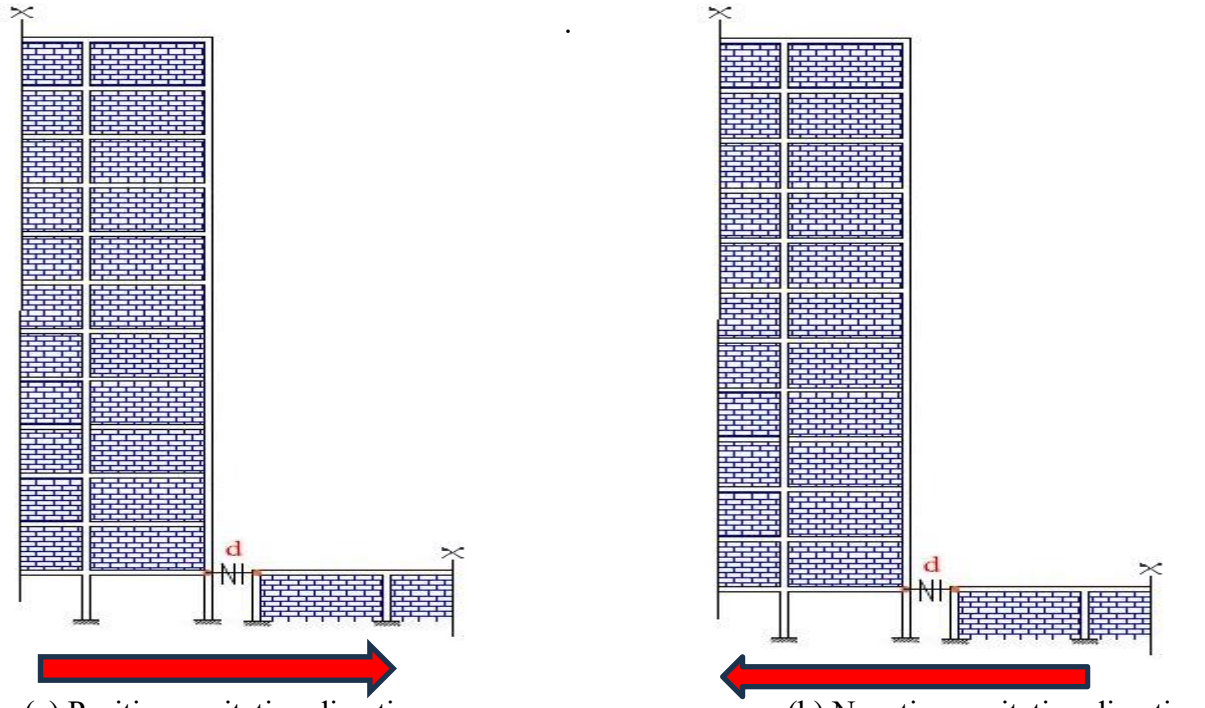

(a) Positive excitation direction (b) Negative excitation direction

Fig. 11 Schematic show the applied directions of every ground motion for Case A pounding (a) positive direction (b) negative direction

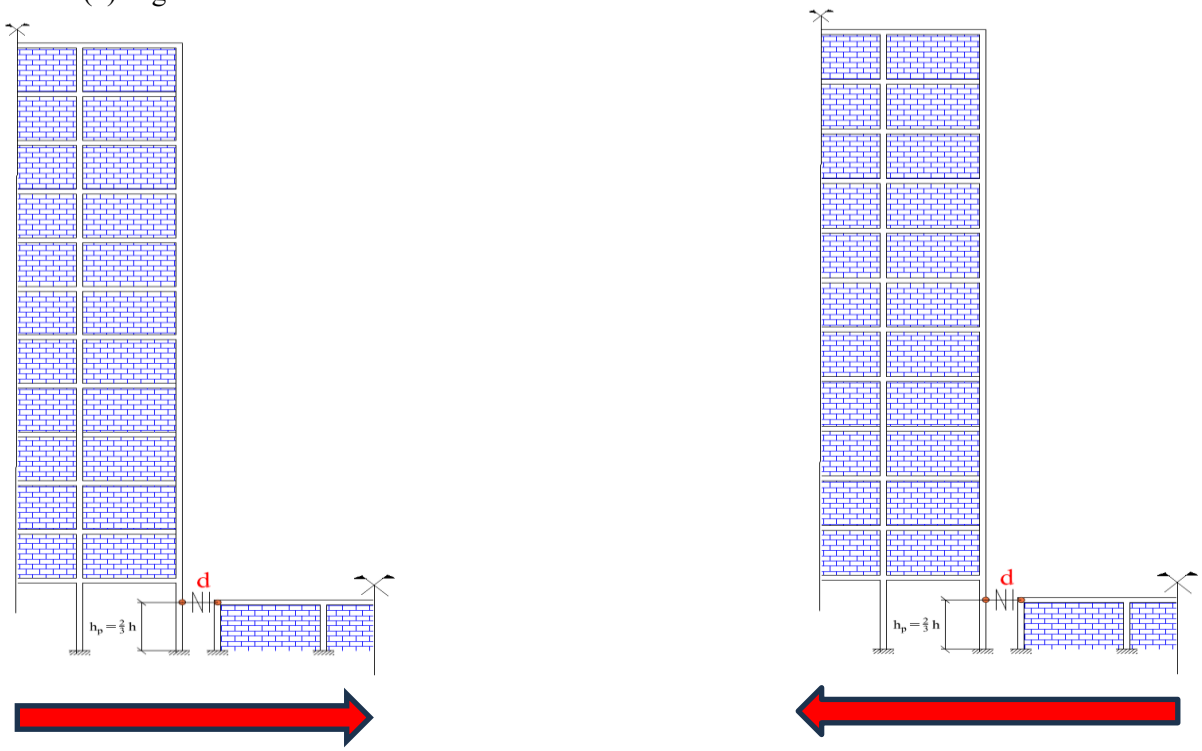

(a) Positive excitation direction (b) Negative excitation direction

Fig. 1 Schematic show the applied directions of every ground motion for Case B pounding (a) positive direction (b) negative direction

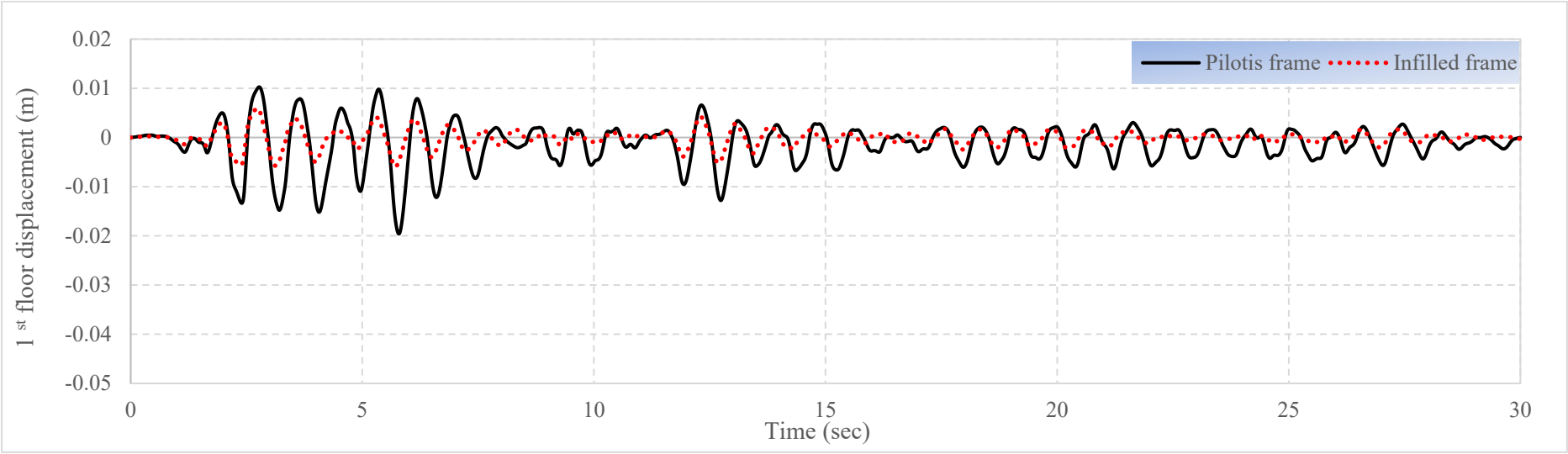

Fig.12 Displacements as function of time history of the first storey under El-Centro record for Case A pounding (excitation applied in positive direction)

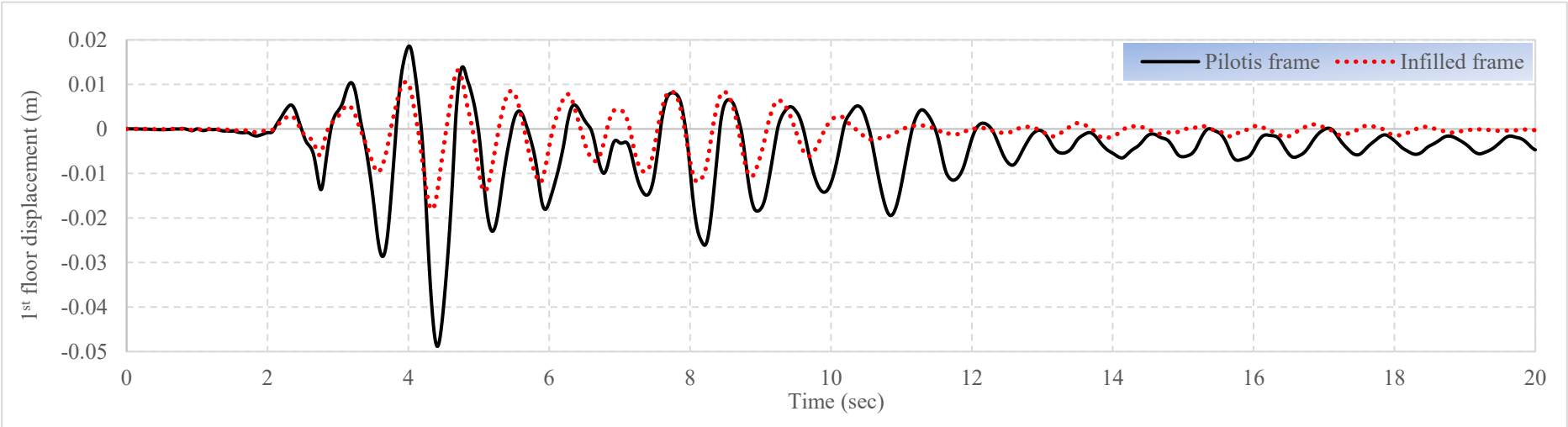

Fig.13 Displacements as function of time history of the first storey under Loma Prieta NF record for Case A pounding (excitation applied in positive direction)

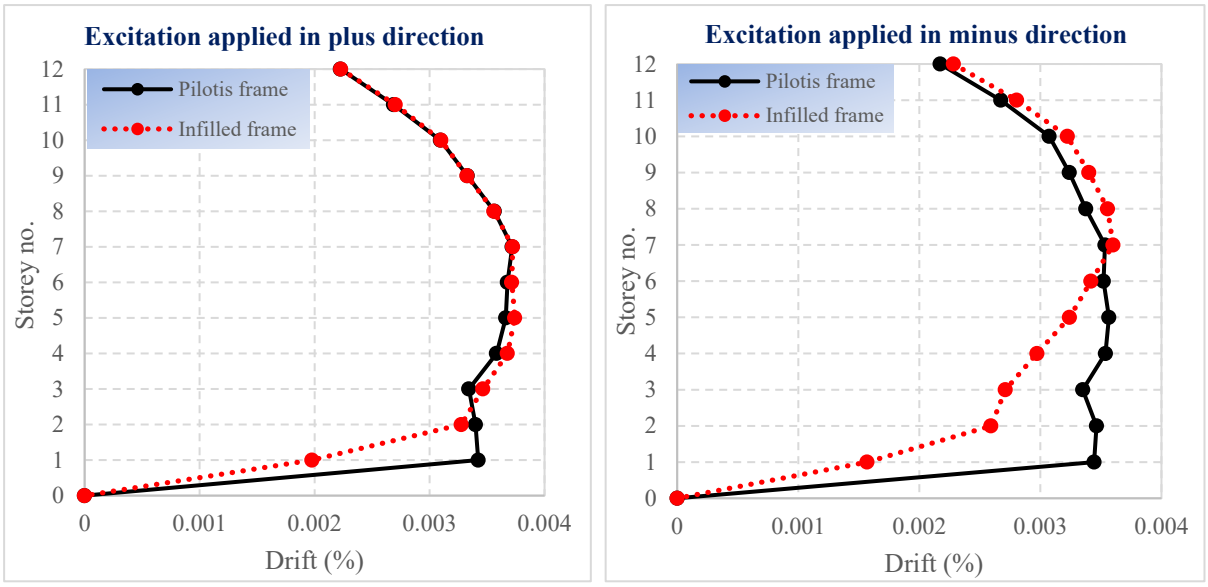

Fig. 6 Maximum inter-storey drifts under El-Centro record applied in positive and negative directions

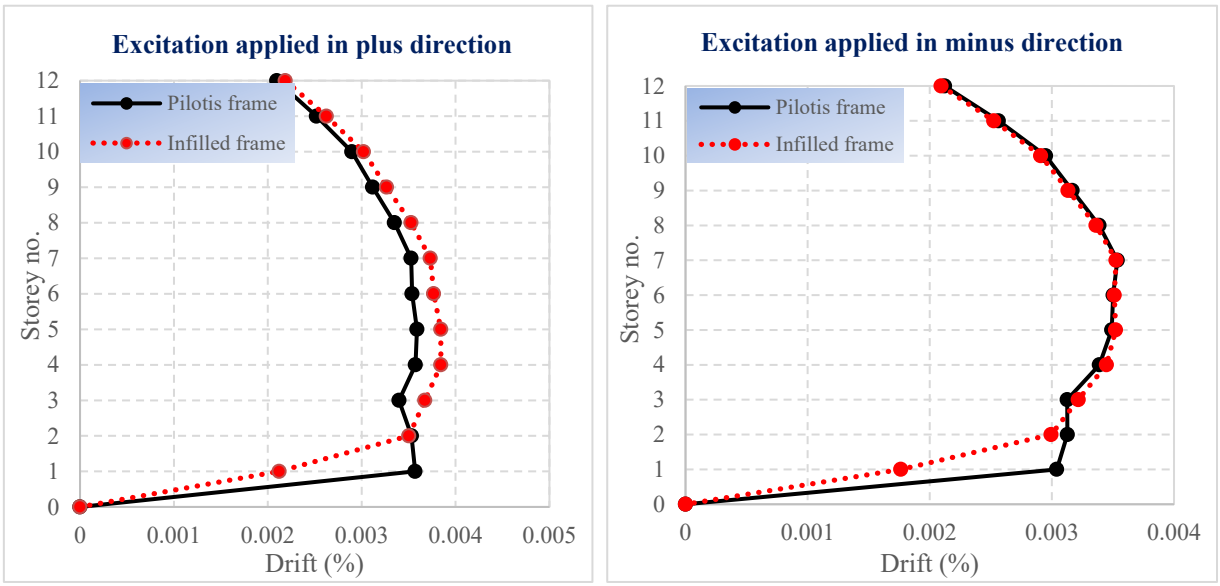

Fig. 15 Maximum inter-storey drifts under Loma Prieta FF record applied in positive and negative direction

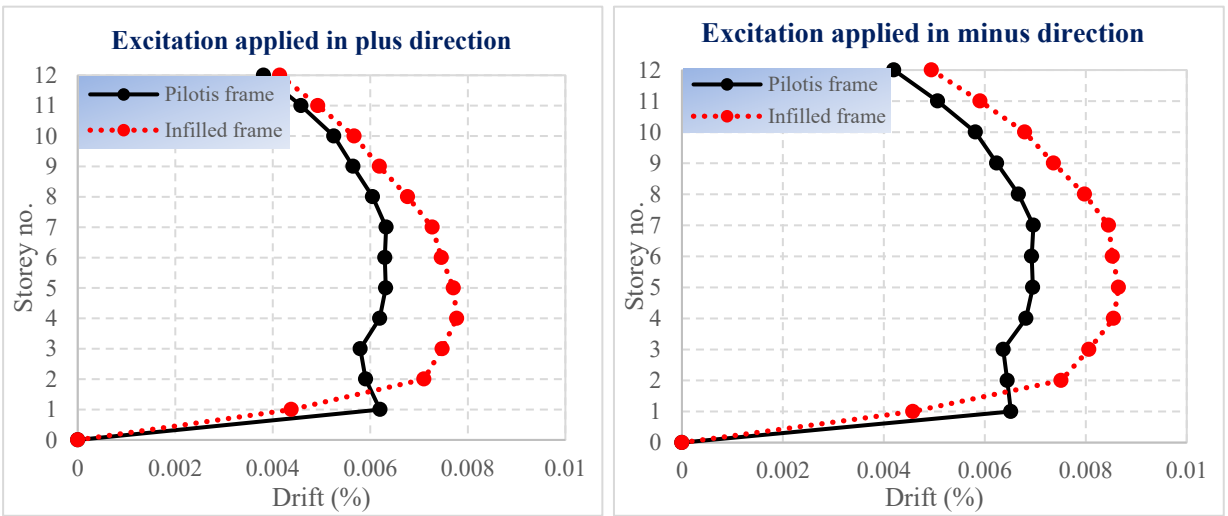

Fig. 16 Maximum inter-storey drifts under Loma Prieta NF record applied in positive and negative direction

The displacements as function of time history of the first storey under El-Centro record and Loma Prieta NF record for Case B pounding (slab-to-column pounding) are represented in figures 18 and 19. The pilotis configuration substantial amplifies the first storey displacement compared to the totally infilled configuration case under the two excitation records. Compared to storey displacement under El-Centro record, the storey displacement induced under Loma Prieta NF record considerable higher regardless of the infilled or pilotis configuration. Overall, there is no major discrepancy between the results of first storey displacement of both totally infilled frame or pilotis frame configuration between Case A (slab to slab pounding) and Case B (slab to column pounding). Just the storey displacement responses of Case B pounding are slightly higher than those resulting from Case A pounding. Also, the inelastic deformation caused by the interaction with the one-storey frame at figure 19 due to Case B pounding is quite higher than those obtained by Case A pounding.

In Figures 20, 21 and 22, the maximum inter-story drifts of the 12- story frame for slab to column pounding Case B under three excitation record applied in both positive and negative directions are also displayed. It was noticed that the pilotis arrangement sharply amplifies the inter-story drift of the first floor and induced considerable permanent deformations because of the pounding. Conversely, there was no significant difference in the inter-story drifts of the frames' top storeys. Furthermore, for all ground motion records, notable variations between the two directions (positive and negative) of input excitation were discovered. Compared to (Case A) slab to slab pounding, the pilots frame configuration of (Case B) slab to column pounding possess an abrupt rise at the designated soft story level. This pattern in drift curves has been noted for the pilotis frame models under all input excitation records. This could be because of the frame with first open storey (pilotis frame) suffering from discontinuities in the strength and stiffness at the first storey level (open storey) compared to the upper storeys. Consequently, the amplification of inter-storey drift for slab to column pounding case (Case B) generally, was more substantial in compared to (Case A) pounding slab to slab pounding case.

6.2.3 Induced pounding force

The induced pounding forces among the 12-storey frame interacting with one-storey structure for slab to column pounding (Case B) at 1st impacted level are represented in figures 23, 24 and 25 for the scenarios of an (a) 12-story totally infilled frame (b) 12- story pilotis frame. Pounding forces were zero when the adjacent buildings were far apart from each other. However, induced pounding forces were under zero when the two adjacent structures came into contact (d=0.00 m). The negative sign represent that the type of pounding forces is compressive. From Figures 23, 24 and 25, under all ground motion records, it is evident that the induced pounding forces were considerably higher in the case of pilotis arrangement (an infill 12-story frame with an open first story) than in the cases of a totally infilled 12-story frame.

The response amplification factor of induced pounding force between the pilotis arrangement and totally infilled frame is about 220%, 212%, and 193% for figures 23, 24 and 25 respectively. The peak response amplification factor of induced pounding force is noticeable under El-Centro ground motion record. In figure 25 the induced pounding forces in pilotis frame vanished after 12 seconds of excitation’s start although, the gap among the adjacent building is zero (buildings in-contact). This limitation of pounding force because of significant permanent deformation (in-elastic deformation) occurred to 12-story building and the adjoined buildings moved apart from each other.

`

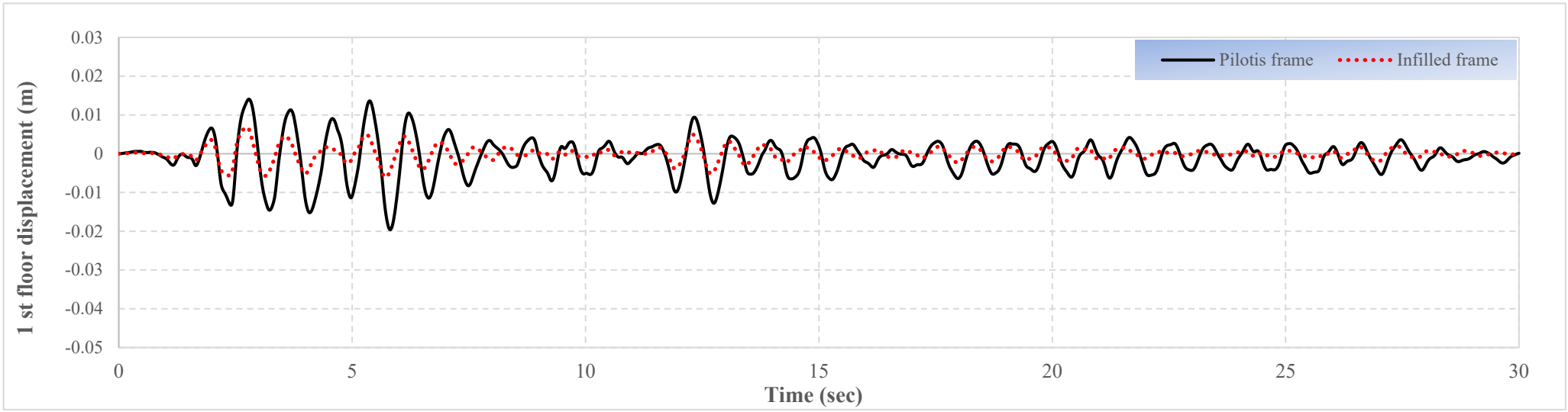

Fig. 18 Displacements as function of time history of the first storey under El-Centro record for Case B pounding (excitation applied in positive direction)

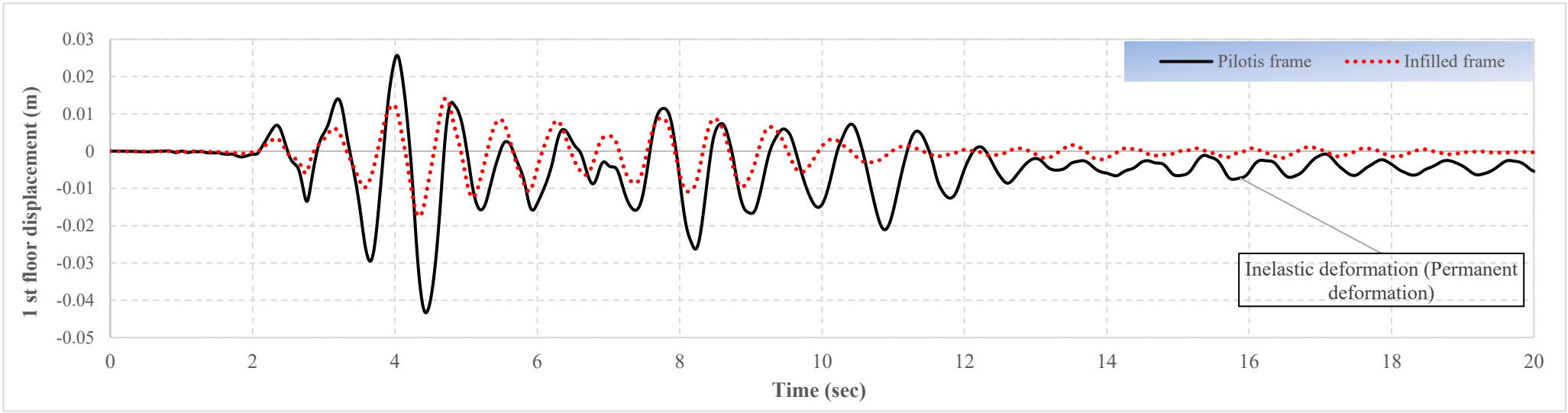

Fig 19 Displacements as function of time history of the first storey under Loma Prieta NF record for Case B pounding (excitation applied in positive direction)

`

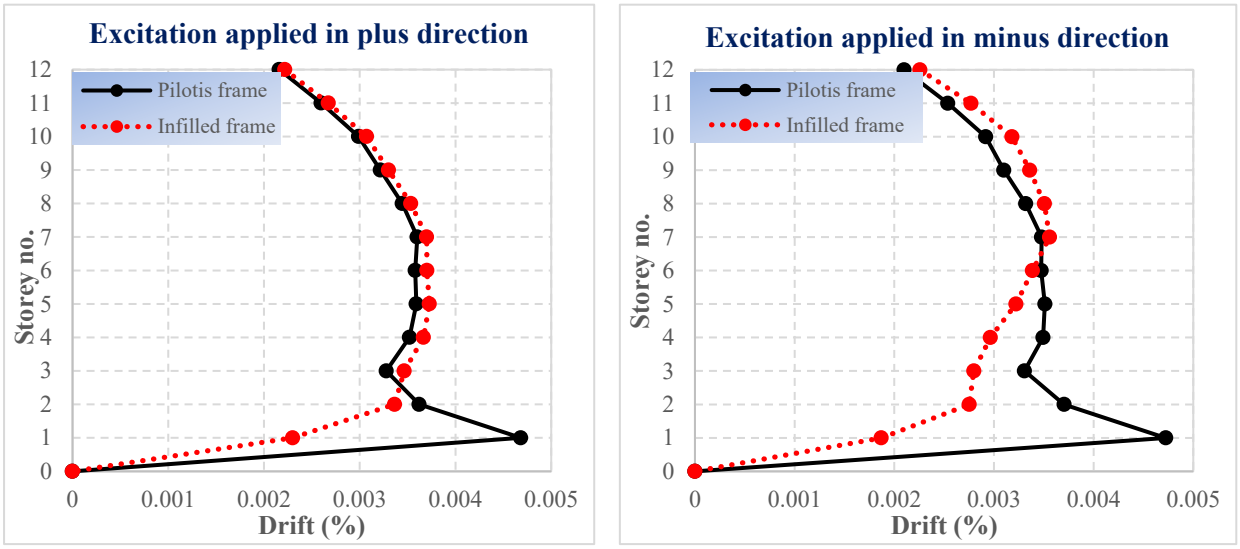

Fig. 20 Maximum inter-storey drifts under El-Centro record applied in positive and negative directions

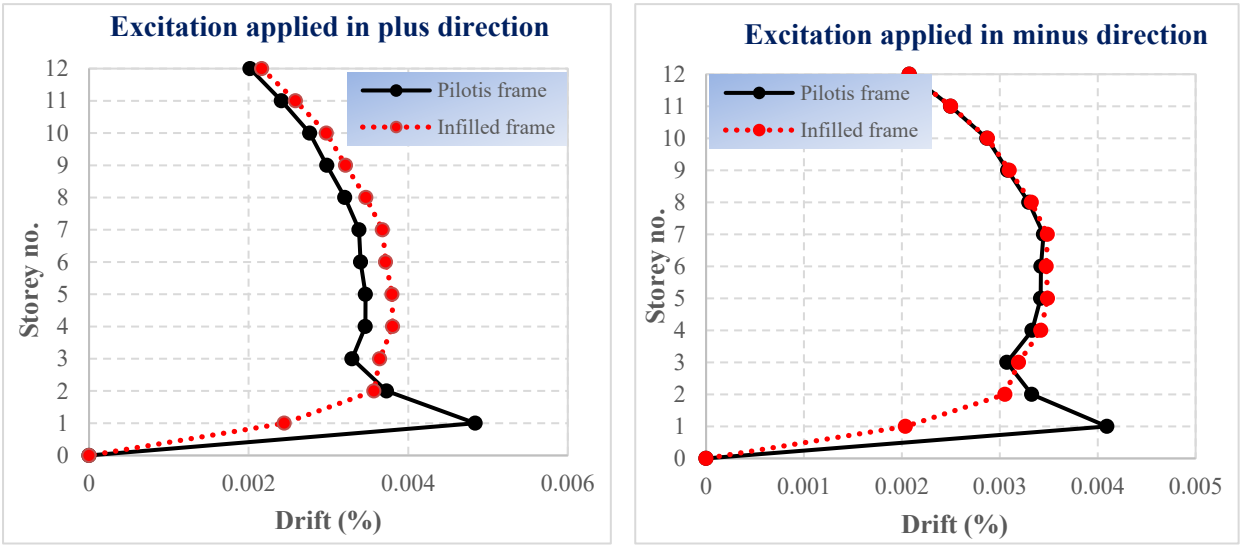

Fig. 21 Maximum inter-storey drifts under Loma Prieta FF record applied in positive and negative directions

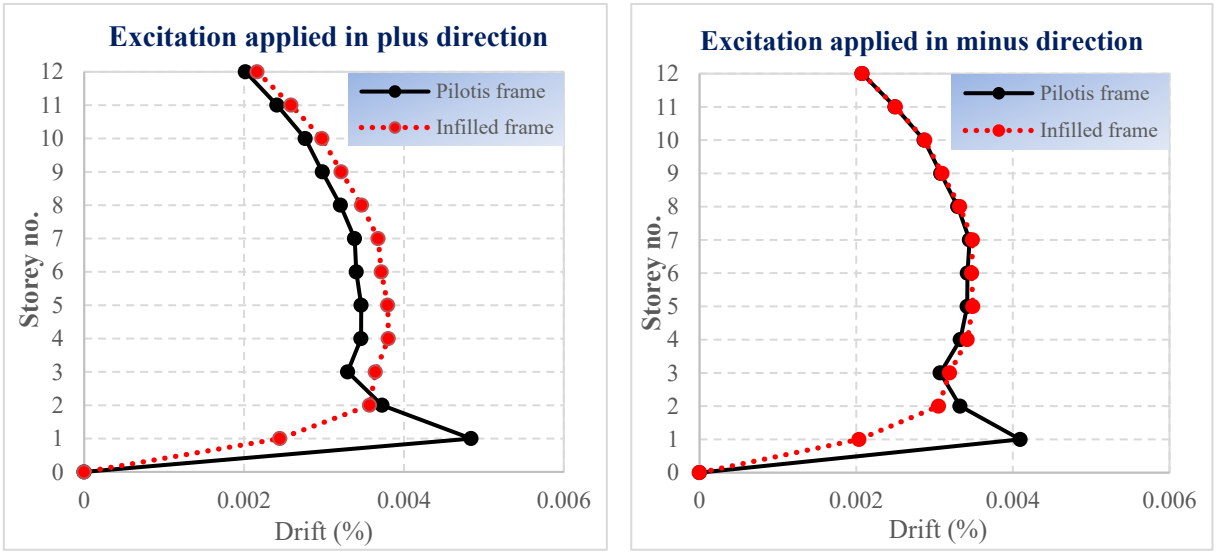

Fig. 22 Maximum inter-storey drifts under Loma Prieta NF record applied in positive and negative directions

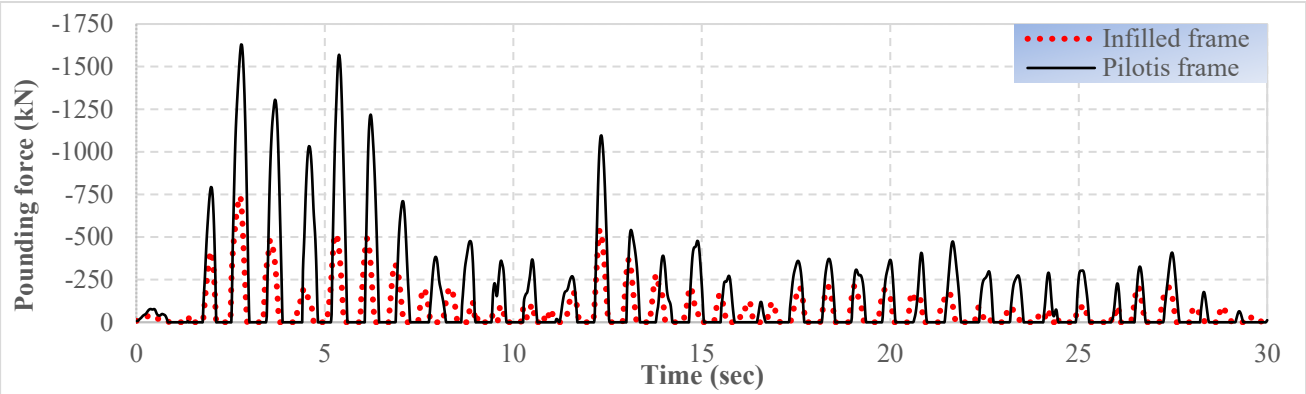

Figure 23 Pounding fore time histories under El-Centro, positive direction, Case B pounding

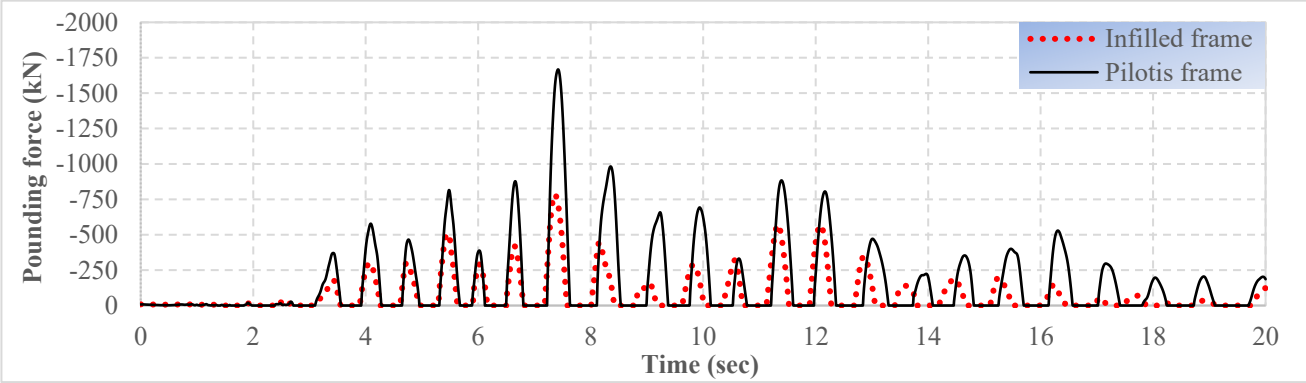

Figure 24 Pounding fore time histories under Loma Prieta FF , positive direction, Case B pounding

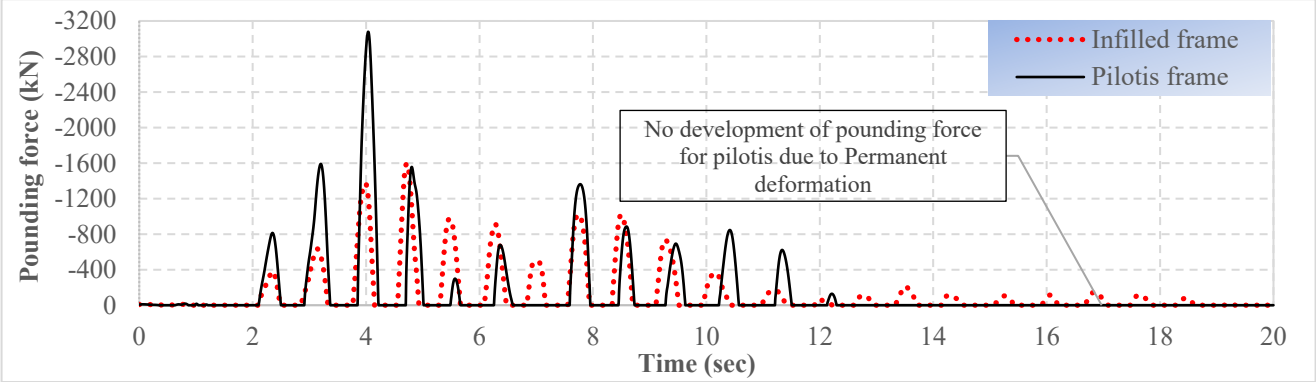

Figure 25 Pounding fore time histories under Loma Prieta NF , positive direction, Case B pounding

6.3 Pounding among the 12-story frame and 6-story frame buildings

The pounding among the 12-story structure and a 6-story structure were investigated as the following:

i. Slab-to-slab pounding (Case A)

ii. Slab-to-column pounding (Case B)

All cases were subjected to three ground motions (El-Centro and near fault and far fault of Loma Prieta) see figure 26.

`

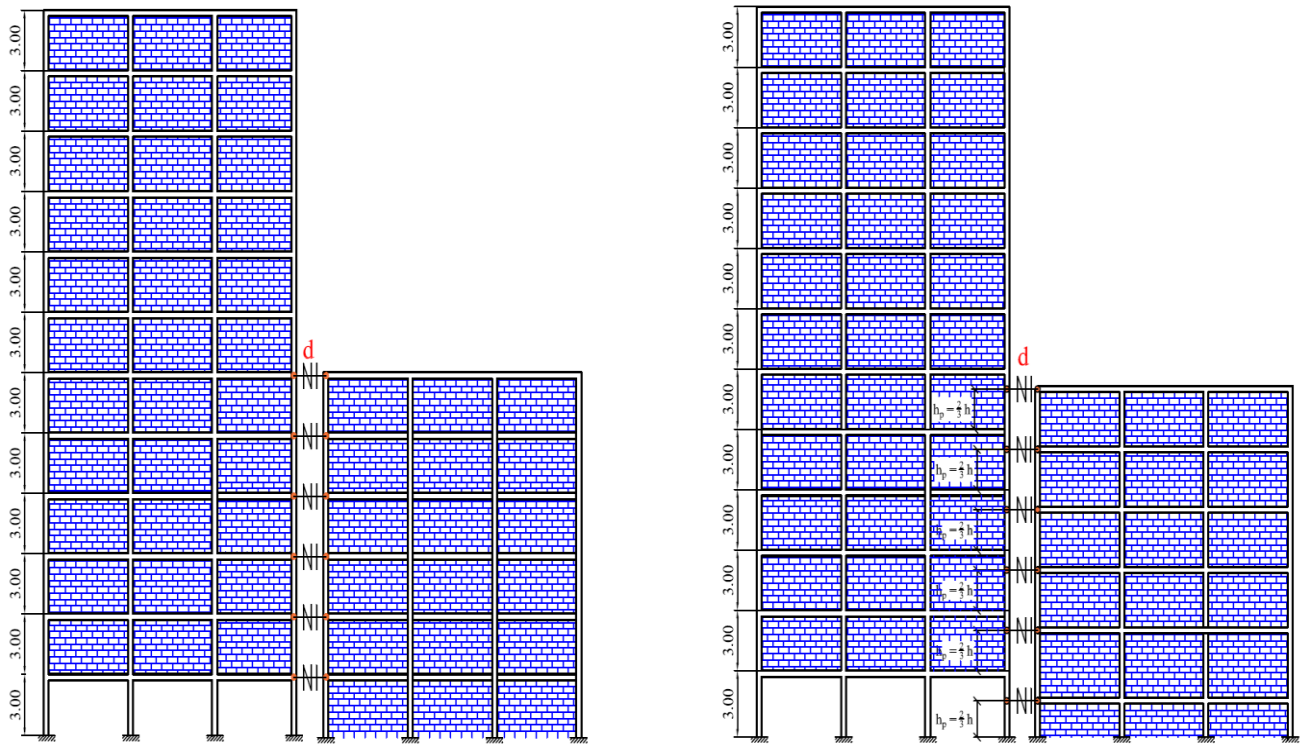

Fig. 26 Seismic pounding between 12-storey pilotis frame and 6-storey infilled-structure (i) Case A or slab-to-slab pounding (ii) Case B or slab-to-column pounding

6.3.1 Maximum inter-story Drifts

Figure 27, 28 and 29 represent the results of slab-to-slab pounding for 12-storey building which interacting with 6- storey building in terms of maximum inter-storey drifts for all considered excitations. Two scenarios were considered in this study: (i) a 12-story frame that was completely infilled, and (ii) a 12-story infilled building with a soft first floor (pilotis). The indication of pilotis frame is the continued black line while the indication of infilled frame is dotted with red line.

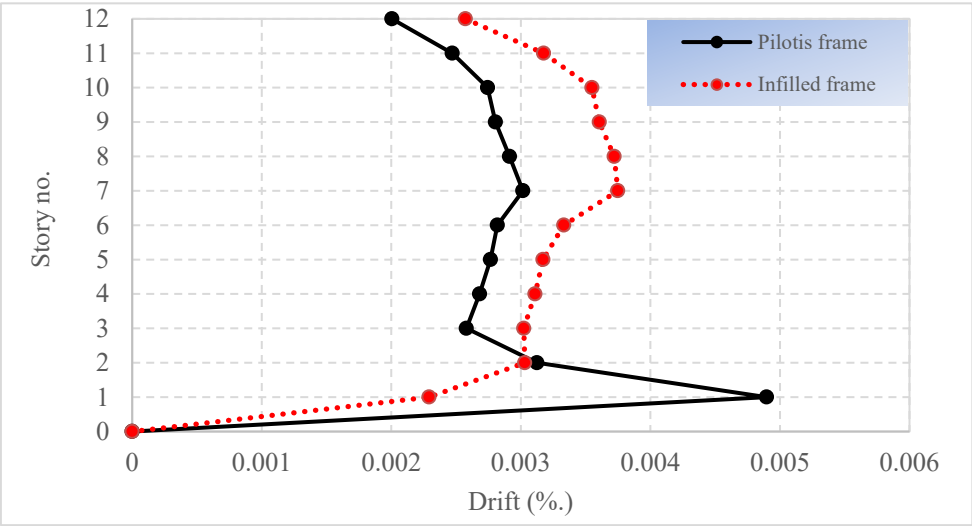

Fi. 27 Maximum inter-storey drifts under El-Centro record for Case A pounding

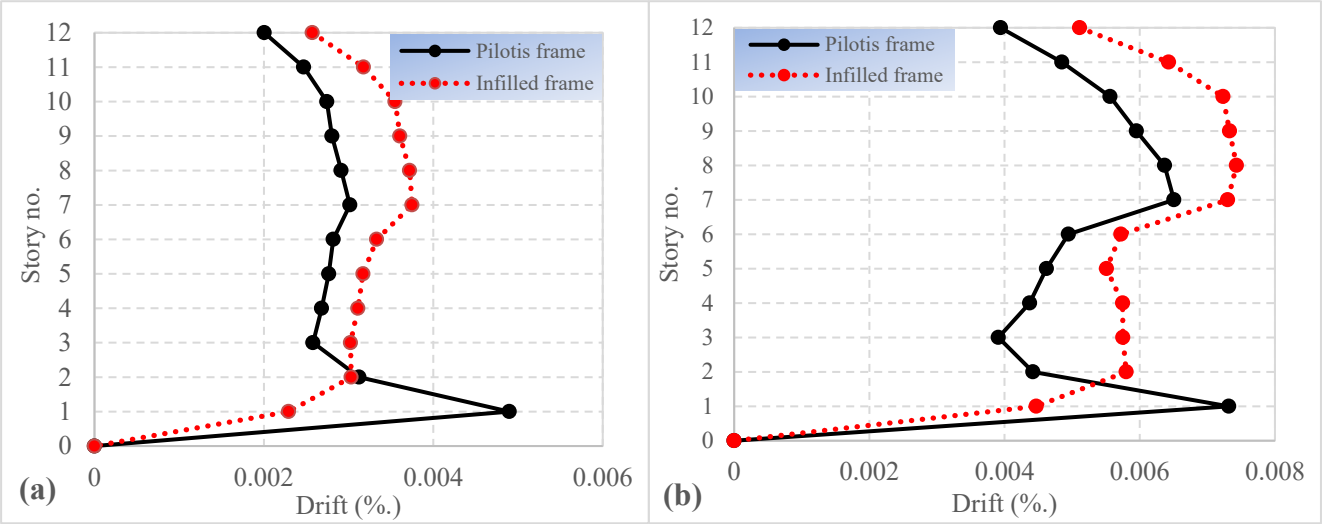

Fi. 28 Maximum inter-storey drifts for Case A pounding (a) under Loma Prieta FF record (b) under Loma Prieta NF record

It was noted from figures 27, 28 and 29 that there is significant increment in the maximum inter-story drift at the first-floor level due to pilotis configuration, while the upper stories show less drifts than infilled configuration due to the pounding. The magnification of story drift at the 1st floor of pilotis arrangement is 220% compared to the totally infilled frame configuration. Also, there are sudden sharp increase in story drifts at the 6th floor level under both configurations of pilotis and totally infilled frame and more notable under Loma Prieta NF record. Figure 28a represents the maximum inter-story drifts under Loma Prieta FF for slab-to-slab pounding (Case A pounding). On contrary to response result under El-Centro record, the stories above the first-floor level show lower story drifts for the pilotis frame configuration compared to the totally infilled frame configuration under Loma Prieta FF record. The magnification of story drift at the first story of pilotis configuration is 215% compared to the totally infilled frame configuration. The increment of story drifts at the impact level of 6th story is not as sharp as the one observed under El-Centro record.

Figure 28b represents the maximum inter-story drifts under Loma Prieta NF for slab-to-slab pounding (Case A pounding). On contrary to response result under El-Centro record, the stories above the first-floor level show lower story drifts for the pilotis frame configuration compared to the totally infilled frame configuration under Loma Prieta NF record. The magnification of story drift at the 1st floor of pilotis arrangement is 164% compared to the totally infilled frame configuration. The significance of input excitation characteristics is highlighted as major influence factor on the responses for example but not limited to story drifts.

6.3.2 Local damage of edge column due to Case B pounding

A crucial issue was the development of plastic hinges of the edge columns located at the first floor of the 12-story building which were stuck by the corresponding slab of the 6-story structure as well as its pilotis configuration. The developing rotation cycles of pilotis frame configuration under the El-Centro and Loma Prieta NF excitations for the edge columns located at the first floor of the 12-story building which were stuck relative to the corresponding one in totally infilled frame configuration are presented in Figures 29 and 30. In particular, moment-rotations response cycles of pilotis frame are illustrated in Figure 29a and the moment-rotations response cycles of the totally infilled frame, in Figure 29b. The

building collision led to transfers additional inertial loads and energy from the adjacent structure to the others. From of particular concern is the possibility of extreme localized damage to structural elements in the region impact zones. The energy balance verifies that in addition to causing local damage, the impact may also alter the response of adjacent buildings depending on their fundamental vibrational properties.

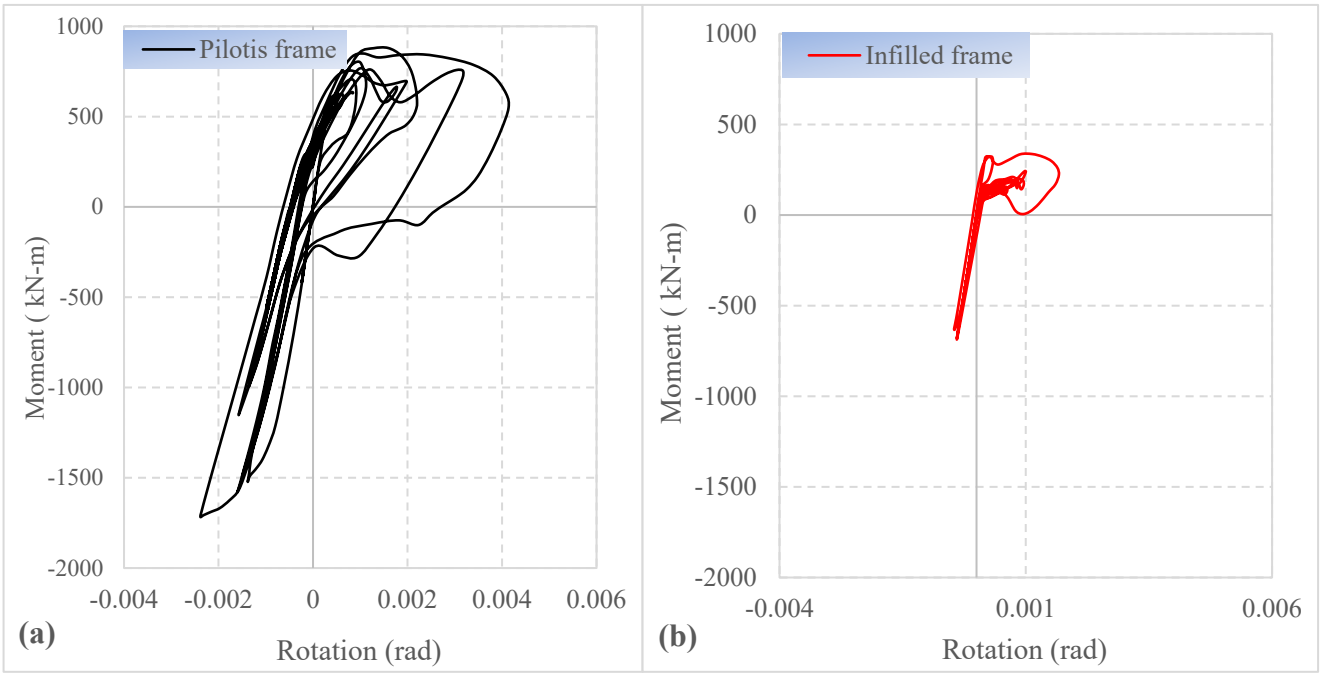

Fig. 29 Cycle loops for the moment-rotation response of top plastic hinge of 1st edge floor column under El-Centro record (a) Pilotis frame configuration (b) Totally infilled frame configuration

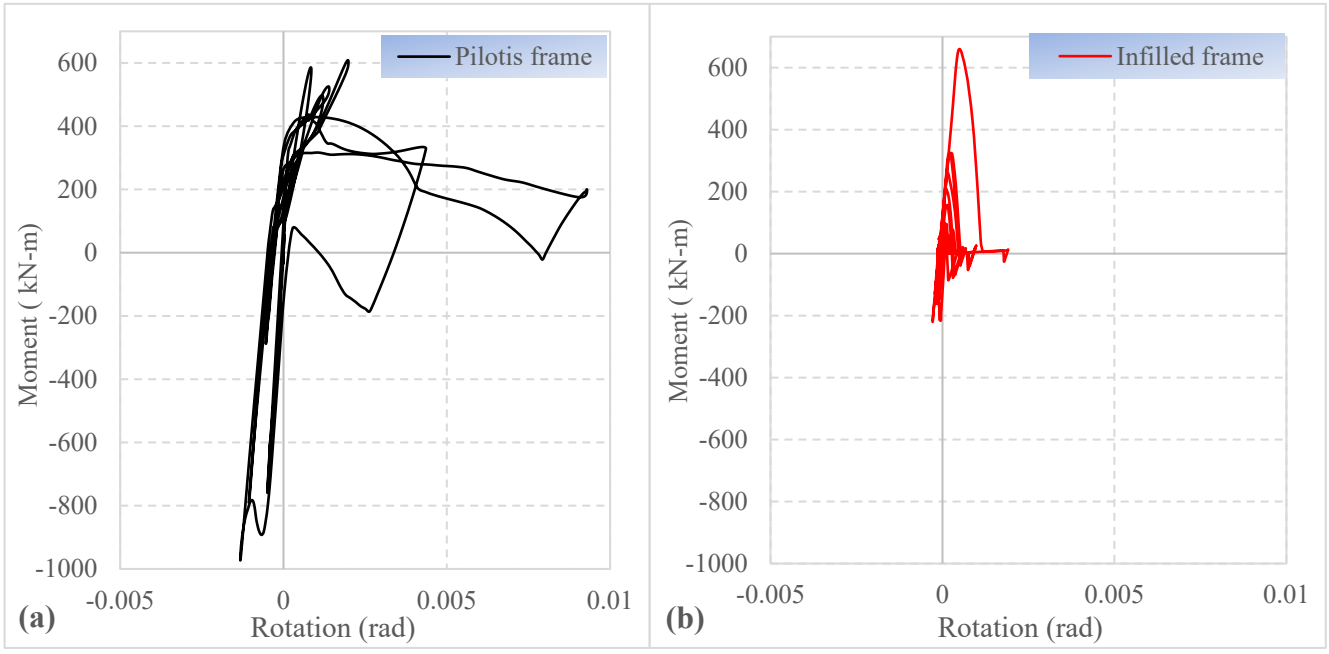

Fig. 30 Cycle loops for the moment-rotation response top plastic hinge of 1st edge floor column of 12-story frame under Loma Prieta NF record (a) Pilotis frame configuration (b) Totally infilled frame configuration

Comparisons between cases of pilotis frame configuration and totally frame configuration with interaction pounding between 12-story and 6- story adjacent buildings show that structural pounding and pilotis configuration can significantly boost the magnitude and level of damage. The results from figures 29 and 30 under demonstrate that collisions cause a substantial rise in the rotations value of the 12-story building in addition, it could lead to an expansion of the damage at the edge column of the taller building. The magnification in rotations of first floor edge column of 12-story building is reach 250% because of the pounding and pilots configuration compared to totally infilled configuration under El-Centro record while the corresponding magnification factor for the same column is 490 %.

6.3.3 Performance level of column hinges

The previous section proves that the pilotis configuration can amplify the maximum rotation of column hinges and as result it could change the performance level of the structural members.

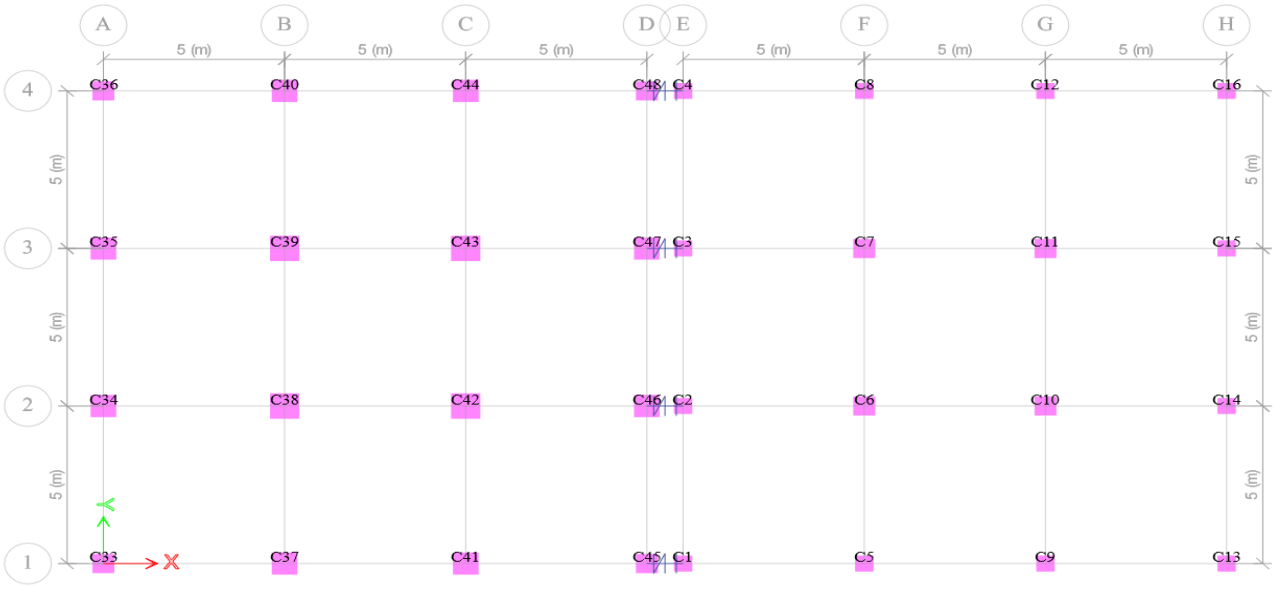

Fig. 31 Column labels plan of the 12-storey frame and 6-storey frame

Table 4 Performance levels of 1st floor column in terms of modelling parameters and acceptance criteria

Building / Story	Col. label	Infilled frame		Pilotis frame	
		Hinge State	Hinge Status	Hinge State	Hinge Status
12STORIES-Story1	C33, C36, C37, C38, C39, C40, C41, C42, C43, C44, C45, C48	A to B	A to IO	B to C	A to IO
	C34, C35, C46, C47	A to B	A to IO	B to C	IO to LS
6STORIES-Story1	C1, C4	A to B	A to IO	B to C	A to IO

Table 4 presents the variance in modeling parameters and acceptance criteria for the first-floor columns, comparing the infilled frame configuration with the pilotis frame configuration. The term hinge state refers to the modeling parameters labeled A, B, C, and D, while the term hinge status refers to the acceptance criteria: Immediate Occupancy (IO), Life Safety (LS), and Collapse Prevention (CP), which describe different damage states. The column locations, indicated by labels, are shown in Figure 31. Columns numbered 1 to 16 belong to the 6-story frame building, whereas columns numbered 33 to 48 belong to the 12-story frame building. For the 12-story frame building, the modeling parameters of all 16 columns changed from a linear state (A to B) to a nonlinear state (B to C) due to the transition from the 12-story infilled frame configuration to the pilotis frame configuration. This change highlights the significant impact of the pilotis configuration and seismic pounding on the columns' performance levels. In contrast, for the 6-story fully infilled frame building, only two columns experienced a change in modeling parameters from the linear state (A to B) to the nonlinear state (B to C). Regarding acceptance criteria, four columns in the 12-story frame building shifted from (A to IO) to (IO to LS), while the acceptance criteria for the 6-story frame building remained unchanged.

7. Conclusions

A detailed numerical analysis of seismic pounding between two adjacent structures was conducted and reported. Specifically, two similar 12-story moment-resisting reinforced concrete frames were designed in accordance with ECP. One frame was fully infilled with masonry, while the other featured an open or soft first story (pilotis). Aside from this difference, the two frames were identical. The 12-story frames were assumed to be in contact (d = 0.00 m) with two other structures: a one-story masonry building and an infilled 6-story frame. Two pounding cases were investigated: slab-to-slab pounding (Case A) and slab-to-column pounding (Case B). The building models were analyzed using nonlinear time-history dynamic analysis under three real recorded accelerograms, namely El Centro and Loma Prieta, representing near-fault and far-fault regions. The input excitation records were applied twice, in both positive and negative directions. The numerical response results included floor displacements, induced pounding forces, inter-story drifts, and moment-rotation response hysteresis loops.

The numerical findings demonstrate the critical role of the pounding phenomenon in the structural response. In particular, this study focuses on the influence of pilotis configuration compared to a fully infilled frame on inter-storey drift and the induced pounding force. The main conclusions drawn from this study are as follows:

1. The seismic response of adjacent buildings can be significantly amplified by pounding.
2. The dynamic characteristics of the input excitation have a significant influence on response quantities.
3. The pilotis configuration amplifies the induced pounding forces and the deformations of the structural components.
4. Pilotis frame significantly increases the maximum inter-story drift at the soft or the open floor.
5. Slab-to-column pounding (Case B) has a significantly greater effect on the response quantities compared to slab-to-slab pounding (Case A).
6. The combination of pounding and the pilotis configuration results in significant inelastic (permanent) deformations.
7. Regardless of whether the adjacent buildings are symmetrical or asymmetrical, it is important to investigate the interaction between structures in both positive and negative directions.
8. The configuration of pilotis can increase the plastic hinge rotations in the open-story columns, which increase the performance level and may also lead to various types of damage.

`

9. The incorporation of infill panels into the MRF model significantly affects the overall structural performance, as it can substantially alter the fundamental natural time period.
10. The pilotis configuration can change the performance level of ground plastic hinges, particularly in taller building compared to shorter ones.

8. Recommendations for future Research Works

The considered building models are symmetrical in plan and a single component of the ground motion is taken in the direction of pounding. However, an accidental torsion as requirement in Section 12.8.4.2 of ASCE 7-10 for buildings is considered. In future studies, the pounding of asymmetric buildings in plan and elevation under 3-components ground motions would be essential to investigated. The current study is theoretically explored using FE software. In future studies, it is crucial to experimentally study these characteristics using shaking table. Consider including retrofit suggestions (e.g., bumpers, isolation joints) for reducing pounding in pilotis buildings; this should be investigated in future studies.

9. Model verification

The findings of previous research in references [6, 12, 17], which indicated that pounding and pilotis configurations may cause significant amplification of the seismic response, are confirmed once again. The performance level of the taller building has increased, while the corresponding performance level for the shorter building has slightly changed. This conclusion is consistent with that obtained in reference [17].

References

1. Arnold, C.; Reitherman, R. Building Configuration and Seismic Design; Wiley: New York, NY, USA, 1982.
2. Rosenblueth, E.; Meli, R. The 1985 earthquake: Cause and effects in Mexico City. Concr. Int. ACI 1986, 8, 23–34.
3. Bertero, V.V. Observation on Structural pounding. In Proceedings of the ASCE-International Conference on Mexico Earthquakes, Mexico City, Mexico, 19–21 September 1986.
4. Maison, B.F.; Kasai, K. Dynamics of pounding when two buildings collide. Earthq. Eng. Struct. Dyn. 1992, 21, 771–786.https://doi.org/10.1002/eqe.4290210903
5. Kasai, K.; Maison, B.F. Building pounding damage during the Loma Prieta earthquake. Eng. Struct. 1997, 19, 195–207. https://doi.org/10.1016/S0141-0296(96)00082-X
6. Manoukas, G.E.; Karayannis, C.G. Seismic Interaction between Multistory Pilotis RC Frames and Shorter Structures with Different Story Levels—Floor-to-Column Pounding. CivilEng 2023, 4, 618-637. https://doi.org/10.3390/civileng4020036.
7. Housing & Building National Research Center (2012) Egyptian code of practice for calculating loads and forces in structural works and building works (ECP 201). Giza,
8. Anagnostopoulos, S.A. Pounding of buildings in series during earthquakes. Earthq. Eng. Struct. Dyn. 1998, 16, 443–456. https://doi.org/10.1002/eqe.4290160311
9. Jankowski, R. Impact force spectrum for damage assessment of earthquake-induced structural pounding. Key Eng. Mater. 2005,293, 711–718. https://doi.org/10.4028/www.scientific.net/KEM.293-294.711

`

10. Jankowski, R. Pounding force response spectrum under earthquake excitation. Eng. Struct. 2006, 28, 1149–1161. https://doi.org/10.1016/j.engstruct.2005.12.005
11. Mouzakis, H.P.; Papadrakakis, M. Three-dimensional nonlinear building pounding with friction during earthquake. J. Earthq. Eng. 2004, 8, 107–132. https://doi.org/10.1080/13632460409350483
12. Moustafa,A., Mahmoud, S.: Damage assessment of adjacent buildings under earthquake loads. Eng. Struct. 61, 153–165 (2014). http://dx.doi.org/10.1016/j.engstruct.2014.01.004
13. Karayannis, C.G.; Naoum, M. Torsion effect due to asymmetric pounding between multistory RC buildings. In Proceedings of the 6th International Conference on Computational Methods in Structural Dynamics and Earthquake Engineering COMPDYN 2017, Rhodes Island, Greece, 15–17 June 2017; Volume 2, pp. 3519–3529.
14. Karayannis, C.G.; Naoum, M. Inter-story pounding and torsional effect due to interaction between adjacent multistory RC buildings. In Proceedings of the 6th International Conference on Computational Methods in Structural Dynamics and Earthquake Engineering COMPDYN 2017, Rhodes Island, Greece, 15–17 June 2017; Volume 2, pp. 3556–3567.
15. Karayannis, C.G.; Naoum, M. Torsional behavior of multistory RC frame structures due to asymmetric seismic interaction. Eng. Struct. 2017, 163, 93–111. https://doi.org/10.1016/j.engstruct.2018.02.038
16. Mahmoud, S.; Genidy, M.; Tahoon, H. Time-History Analysis of Reinforced Concrete Frame Buildings with Soft Storeys. Arab. J. Sci. Eng. 2017, 42, 1201–1217. https://doi.org/10.1007/s13369-016-2366-1
17. Abbas Moustafa, Magdy Genidy, Hesham Tahon and Hany Ragab (2025). Pounding interaction among adjacent MRF multi-storey buildings and associated performance levels under strong ground motion. 10.21608/erj.2025.375005.1226.
18. Computers and Structures Inc. (CSI) (2022) ETABS2022 Ultimate C v20.3.0 Build 2929. Computers and Structures Inc., Berkeley.
19. A.K. Chopra, Dynamics of structures, 3rd edition, Prentice Hall, NJ, 2006.
20. Mander JB, Priestley MJN, Park R (1988) Theoretical stress–strain model for confined concrete. J Struct Eng 114(8):1804–1826.
21. FEMA-356. Prestandard and commentary for the seismic rehabilitation of buildings. Federal Emergency Management Agency. Washington DC: 2000.
22. ASCE41-17. Seismic Evaluation and Retrofit of Existing Buildings In: ASCE/SEI standard 41-17. American Society of Civil Engineers. Reston: 2017. 10.1061/9780784414859.
23. Watanabe G, Kawashima K (2004) Numerical simulation of pounding of bridge decks. In: The 13th world conference on earthquake engineering, Vancouver, BC, Canada.
24. Maison BF, Kasai K (1992) Dynamics of pounding when two buildings collide. Earthq Eng Struct Dyn 21:771–786.
25. Anagnostopoulos SA (1988) Pounding of buildings in series during earthquakes. Earthq Eng Struct Dyn 16:443–456.
26. Kawashima K, Shoji G (2000) Effect of restrainers to mitigate pounding between adjacent decks subjected to a strong ground motion. In: 12th world conference on earthquake engineering, New Zealand, Auckland, Paper no. 1435.

27. Guo A, Cui T, Li H (2012) Impact stiffness of the contact-element models for the pounding analysis of highway bridges: experimental evaluation. J Earthq Eng 16(8):1132–1160.
28. Jankowski R (2006) Pounding force response spectrum under earthquake excitation. Eng Struct 28:1149–1161.
29. Shakya K, Wijeywickrema AC, Ohmachi T (2008) Mid-column seismic pounding of reinforced concrete buildings in a row considering effects of soil. In: 14th WCEE, Beijing, Paper ID 05-01-0056.
30. Karayannis, C.; Kakaletsis, D.; Favvata, M.J. Behavior of bare and masonry infilled R/C frames under cyclic loading. Experiments and Analysis. WIT Trans. Built Env. 2005, 84, 429–438.
31. Pacific Earthquake Engineering Research Center (PEER) (2013). PEER NGA-West2 database. PEER report 2013/03, Pacific Earthquake Engineering Research Center, University of California, Berkeley.

`